

Response to reviewers: Influence of ENSO on North American subseasonal surface air temperature variability (wcd-2020-22)

We are grateful to the two reviewers for providing valuable comments on our manuscript. Our responses are included below.

Response to reviewer 1

We thank the reviewer for taking the time to assess our manuscript and for providing valuable comments. As suggested by the two reviewers, we modify our analysis to focus on tropical Pacific SST variability instead of the whole NH Pacific. Our results are not sensitive to the change of domain and thus our conclusions remain the same. Our replies to the reviewer's comments are shown in blue below. Line numbers refer to the manuscript with tracked changes.

In this study, the authors investigated the influence of ENSO on North American subseasonal surface air temperature (SAT) variability in boreal winter. The dominant mode of covariability between 10-60 day band-pass filtered SAT variability and winter-mean SST over the North Pacific sector was identified using an SVD analysis. It was found that La Nina conditions tend to enhance the subseasonal SAT variability over western North America. Detailed analysis of energetics of subseasonal eddies was carried out. The results are in agreement with previous studies. An interesting finding is that changes in vertical structure of the subseasonal anomalies are important for energy conversion through heat fluxes. The topic is interesting and the manuscript is in general clearly written. It may contribute to the understanding of subseasonal SAT variability and its related extreme events. I think this manuscript is publishable subject to some minor revisions.

Specific comments: 1. This study deals with ENSO influence on the North American subseasonal SAT. However, the area chosen for the SST in the SVD analysis is mainly the North Pacific region. The resulting seasonal mean SST anomaly has a strong signal in the North Pacific, which may not be related to ENSO. It would be more reasonable to use the tropical Pacific area, e.g., 30S-30N.

Thank you very much for the comment. As suggested, we modify the sector over which SST is used for the SVD analysis. By limiting the domain to 20S-20N, we now focus solely on tropical Pacific variability. Please note that extratropical SST anomalies are still present, albeit weaker than the equatorial anomalies (Fig. 2). This is not surprising since tropical SST variability related to ENSO is accompanied by SST variability in the extratropics (e.g., Deser et al. 2010).

2. In the paragraph starting from line 221 and Fig. 7, it should be justified why the two points, Alaska and Colorado, are selected to perform the lagged regression calculation. Is it based on the variance? Are the results sensitive to the choice of base points? Are these subseasonal patterns consistent with previous studies (e.g., Lin 2015)?

We add at line 293: "These locations are chosen because SVD1 has a large impact on SSV over these sectors (Fig. 2)". We also add at line 304: "As illustrated in Fig. 8, atmospheric circulation patterns associated with localized SAT variability are quite sensitive to the reference location. These patterns share similar features, such as their spatial scale and meandering, with the circulation anomalies associated with the leading modes of SAT variability (Lin 2015). The exact location of their cyclonic and anticyclonic centres of action are however not the same. They may correspond to modes of lesser importance or combinations of the leading modes. Other reference locations over North America were assessed and revealed different circulation anomalies (not shown)."

3. What is the implication of this study to subseasonal predictions of surface air temperature in North America?

We add the following discussion at the end of our manuscript: “Concerning subseasonal predictions, our results suggest that predictive skill over North America may be deteriorated during La Niña winters due to enhanced energy conversion to subseasonal variability and, as a consequence, increased atmospheric internal variability over the sector. This is in agreement with the overall less skillful predictions achieved during the negative phase of the PNA (Lin and Derome 1996; Sheng 2002) which, in terms of extratropical mean flow changes, is to some extent similar to the extratropical response to La Niña.”

Reference: Lin, H., 2015: Subseasonal variability of North American wintertime surface air temperature. *Climate Dyn.*, 45, 10.1007/s00382-014-2363-6, 1137-1155.

References

Deser, C., M. A. Alexander, S.-P. Xie, and A. S. Phillips, 2010: *Sea Surface Temperature Variability: Patterns and Mechanisms*. 115–143 pp.

Lin, H., 2015: Subseasonal variability of North American wintertime surface air temperature. *Clim. Dyn.*, 45, 1137–1155, <https://doi.org/10.1007/s00382-014-2363-6>.

—, and J. Derome, 1996: Changes in predictability associated with the PNA pattern. *Tellus A Dyn. Meteorol. Oceanogr.*, 48, 553–571, <https://doi.org/10.3402/tellusa.v48i4.12139>.

Sheng, J., 2002: GCM experiments on changes in atmospheric predictability associated with the PNA pattern and tropical SST anomalies. *Tellus A Dyn. Meteorol. Oceanogr.*, 54, 317–329, <https://doi.org/10.3402/tellusa.v54i4.12153>.

Response to reviewer 2

We thank the reviewer for providing useful comments which have helped us improve our manuscript. As suggested by the two reviewers, we modify our analysis to focus on tropical Pacific SST variability. Our results are not sensitive to the change of domain and thus our conclusions remain the same. Our responses to the comments are written in blue below. Figure numbers refer to the new figure set which includes a new figure at the beginning.

This study is interested in the influence of ENSO on subseasonal variability in North American SAT during the winter season. Previous studies found that La Nina conditions are associated with enhanced subseasonal SAT variability (SSV) over western North America. Here, the authors use SVD, regression/correlation and composite analyses to investigate how ENSO affects subseasonal variability through modulation of subseasonal eddies - specifically, via changes to the vertical structure of the eddies which have bearing on the amount of baroclinic energy conversion that occurs. The subject is interesting and relevant to improving our understanding of climate dynamics, as improving near-term climate predictions, and better understanding the large-scale conditions for extreme events. I feel this manuscript could represent a valuable contribution to these areas of research, but would first require substantial revisions to address a number of scientific and methodological issues that are a bit unclear.

First and foremost, while the abstract sounds nicely focused, the rest of the paper seems to mix together a number of different research questions without quite giving the reader enough guidance to connect them (see especially comment #1). The presentation is generally fine, and figures are of good quality, although the captions should include more details so that the reader need not go back to the text to look up information, abbreviations, etc.

MAJOR COMMENTS

The setup of a clear, motivating question in the introduction is not quite there. There seem to be several trains of thought, including the influence of ENSO on SSV, the link from SSV to extremes, and the mechanisms by which ENSO affects SSV, but they are not well connected and in some cases, we seem to be missing some background information needed to make this connection.

Some specific comments:

- Is the ENSO-related SSV signal just part of the PNA-related SSV? if not, how is it different?

This is a good point. We now note at line 221 that the winter-mean response is “more similar to the extratropical response forced by ENSO than the internally-generated PNA (Straus and Shukla 2002)” and we add the following discussion in the conclusion (line 424) :“ ENSO-induced anomalies of the extratropical circulation share some similarities with the PNA, but they are not identical (Straus and Shukla, 2002). The anomalies are known, for instance, to be projected also onto the Tropical Northern Hemisphere (TNH) pattern (Soulard et al., 2019; Trenberth et al., 1998). It remains unclear at this stage whether the modulation of baroclinic energy conversion is achieved through the projection of the extratropical response on the internally-driven PNA or TNH. We nevertheless speculate that it may be achieved primarily through the PNA, since important modulations of baroclinic energy conversion take place over the western North Pacific, where the PNA has a greater influence on the winter-mean flow. A more detailed investigation of the modulations of subseasonal energy sources by internally-generated interannual variability should be the topic of a future study”.

In summary, we believe that while it is interesting to understand how the teleconnections onto which ENSO’s extratropical response is projected modulate subseasonal variability, it is out of the scope of the

present study and should be the topic of a standalone paper on internally-generated variability. Not only the PNA but also the TNH and other teleconnections affecting the North Pacific sector should be investigated.

- How important is the portion of extratropical SSV related to ENSO? It seems key to establish this upfront, since later on in Fig. 10, you show an SSV signal unrelated to your ENSO index (SVD1) that is both substantial in amplitude and very similar to the ENSO-related signal. It would also be nice to show the SSV climatology for reference, perhaps early on in the results section, since this is a field many readers will not be so familiar with.

Thank you for the comment. Instead of showing the percentage of the climatology that these ENSO-related variations represent, we show the percentage of local total interannual variance explained by ENSO (Fig. 2a). The percentage explained is up to about 10% which contrasts with the variance explained by the ENSO-unrelated signal which explains up to 50% of the total variance (Fig. 11a). These percentages of variance explained are now indicated in the manuscript.

Also, we add a new figure (Fig. 1) to show the basic climatological properties of SAT. The climatologies of SAT and SSV are now discussed at lines 184-203.

- And perhaps even one step before this, how important is SAT variability in the 10-60 day band?

We add a discussion (lines 192-199) on the importance of SAT variability in the 10-60 day band by contrasting variability at this time scale with high-frequency variability (2-8 days) which is more thoroughly studied. To this end, the climatology of high-frequency SAT variability is shown in Fig. 1c.

- The paragraph starting on L42 seems to be off-topic - if this is meant to relate to the issue of extremes, the connection needs to be made better. In general, the parts of the manuscript dealing with extremes seems like somewhat of an afterthought - it probably should be either expanded or de-emphasized.

The reason we discuss blocking there is to illustrate, with a specific event of subseasonal time scale, how ENSO can modulate subseasonal variability and associated weather impacts. Such influence has rarely been discussed for general subseasonal variability, but abundant literature investigated this influence in the context of atmospheric blockings. We believe that our discussion with linkage to extreme events in referring to blocking is relevant to subseasonal variability, because extremes are, by definition, associated with highly anomalous, and thus variable, weather. We nevertheless agree that this discussion could be connected better with the preceding part of the introduction. We try to improve the link with the preceding paragraph by writing (line 45): "This ENSO influence on intraseasonal variability may be achieved in part through modulation of the frequency of blocking events..." Afterward, we introduce in more detail their relationship with weather extremes.

We believe that the section about the impact of ENSO on extremes, although brief, may be of interest to some readers. We consider that it is important to illustrate that subseasonal variability is not the only factor controlling extremes. Its combined influence with ENSO-related winter-mean changes in temperature is important. Nonetheless, we de-emphasize this aspect by removing the last paragraph of the introduction that summarizes this finding.

Also, the topic sentence seems to say there is a clear association between ENSO and blocking, while later in the paragraph, we see that the association is not clear.

We soften the topic sentence and discuss more extensively a possible reason for the different conclusions among studies (line 56): “The studies that have defined blocking events as prominent anomalies have reported an increase in the frequency of blocking during La Niña (Renwick and Wallace 1996; Barriopedro and Calvo 2014; Chen and van den Dool 1997), which is in agreement with the aforementioned changes in intraseasonal variability. Considering the link between blocking and weather extremes, this suggests a potential increase in the frequency of extreme cold episodes on subseasonal time scales during La Niña.”

- The paragraph starting on L60 - I’m having some trouble with the logical flow in the first few sentences.

We rewrite the first few sentences to improve clarity (lines 71-75).

- I’m not sure how familiar most readers are with the term "subseasonal eddies".

We now define what we mean by subseasonal eddies at line 96: “atmospheric circulation anomalies on subseasonal time scales, hereafter referred to as subseasonal eddies”.

2. The title and abstract talk about ENSO’s influence on SSV, but the "first step" (L73) is identifying the dominant mode of covariability between North Pacific SST and SSV. Why not use an ENSO index - either one of the standard ones in Table 1, or an EOFbased index of tropical Pacific SST (Takahashi et al., Cai et al.)? I see that the SVD1 produces indices that are well correlated with ENSO, but I don’t understand the point of using this over using actual ENSO indices (perhaps there is a good reason but I’ve missed it, in which case it should be better explained). Even if one were to use an SVD, would it not be better to choose a tropical Pacific box for the SST field? It’s been shown that including the North Pacific mixes frequencies and forcing source regions (Wills et al.).

- Cai et al. (2018): Increased variability of eastern Pacific El Niño under greenhouse warming. *Nature*, 564

- Takahashi et al. (2011): ENSO regimes: Reinterpreting the canonical and Modoki El Niño. *Geophys. Res. Lett.*, 38, L10704

- <https://agupubs.onlinelibrary.wiley.com/doi/full/10.1002/2017GL076327>

Thank you very much for the comment. We focus our new analysis on tropical SST variability by limiting the SVD domain to 20°S-20°N. Our results are not sensitive to this modification and our general conclusions remain the same.

We now better motivate our approach in the Methods section (lines 111-119): “One approach to investigating the influence of ENSO on subseasonal SAT variability is to start from classic ENSO indices (see the next section). The individual indices, however, represent different “flavours” of ENSO that may exert distinct impacts on North-American subseasonal SAT variability. Instead of repeating our analysis for all these indices, we identify, via singular value decomposition (SVD) analysis (Bjornsson and Venegas, 1997; Bretherton et al., 1992), a particular “flavour” of tropical Pacific SST variability that is optimally related to subseasonal SAT variability over North America. Identifying this optimal influence is not only important to better predict SAT variability from SST anomalies but also contributes to improving the clarity of the rest of our analyses by focusing on the strongest statistical connection.”

3. I like the dynamical line of investigation regarding why subseasonal eddies may be more "active" during La Nina. I think the argumentation could be made more convincing, and this would really

strengthen the paper as a whole. First, the connection from subseasonal SAT variability to the subseasonal eddies should be made clearer in the text (just a few lines of explanation to help the reader interpret the figures).

We add a discussion to justify why we study energetics to better understand SAT variability at lines 230-232): “The rationale is that SSV is produced by weather systems (or eddies) that have deep structures within the troposphere and thus better understanding of interannual fluctuations of SSV can be acquired through investigating year-to-year changes in processes that energize these eddies”.

Second, Fig. 8 is not so compelling as a demonstration that differences in the vertical structure of the eddies are key. Some suggestions: (a) show a larger longitudinal range that include all the positive/negative centres of action seen in Fig. 7, so we see the change in vertical structure systematically with each one, (b) show barotropic energy conversion with height, so we see the big increases where the temperature and Z fields are most offset.

We keep our focus close to the reference latitude because it is where we have greater confidence about the structure of the subseasonal eddies. Further away from the reference time series, where remote anticyclonic and cyclonic anomalies are located, correlations and regressions decrease substantially which means we do not have as much confidence in the identified structure since the signal to noise ratio is low. This is why we have chosen a reference time series located in the region of large modulation of CP, and not over North America, for this analysis. We add (line 320): “For a robust illustration of the structure of eddies over that sector, it is preferable to use a local reference grid point in this analysis (as indicated with a green circle in Figs. 3c and 6). Eddy structures constructed from remote reference SAT time series over Alaska and Colorado (Fig. 8) do exhibit signals over the North Pacific, but the correlations are substantially weaker which indicates a low signal to noise ratio.” In Fig. 8, we add the heat fluxes associated with subseasonal eddy structures to illustrate how the overall contributions to poleward heat fluxes are enhanced in $SVD1_{SST} > 1$ and add the following discussion (line 330): “The net meridional heat fluxes associated with these structures (Figs. 9c-d) are obviously larger for $SVD1_{SST} > 1$ due to marked enhancement (approximate doubling) of poleward heat transport to the west of the reference longitude, which cannot be offset completely by a slight increase in the southward transport to the east

4. Some of the analysis choices seem rather arbitrary, and need to be better explained. Also the analysis itself. Some examples, but not exhaustive:

- regions for the SVD (the SSV box is probably related to target area and climatological field, but what about SST? see comment #2)

In our revised manuscript we limit the SST domain used for the SVD analysis to 20°S-20°N following the reviewers’ comments. This is motivated by our goal to investigate the influence of tropical Pacific variability on North American SSV.

- locations for temperature regressions in Fig. 7

The reference locations used for the regressions shown in Fig. 8 are now indicated with magenta Xs.

- location for Z regressions in Fig. 8. Presumably, we want to look at the eddies responsible for SAT variability such as that seen in Fig. 7? It would be helpful to justify this point and mark it on one of the maps.

The reference location used for the regressions shown in Fig. 9 is now indicated with green circles in Figs. 3 and 6.

- what frequency data is used for the various analyses? Presumably daily or 6-hourly for SSV that is then band-pass filtered? The SVD looks to be using monthly or seasonal averages? What about in the regressions for vertical structures?

We now indicate that we use 6-hourly data for SSW and that the standard deviation is taken over DJF. The section describing the SVD analysis (2.2) states that winter-mean SST is used. We add that the regressions for vertical eddy structures are based on 10-60 day bandpass filtered data.

- how are warm/cold extremes identified?

The definition of cold/warm extremes is described in section 3.5: "Cold (warm) extreme days are defined as the days when 10-day lowpass-filtered SAT anomaly falls below (rises above) the 5th (95th) percentiles at each grid point over the 58 winters. Their frequency, calculated as the percentage of winter days each year, is then regressed onto the $SVD1_{SST}$ time series".

- how are u , v , T defined?

We add in section 2.4 that a 10-day high-pass filter is used.

- Fig. 7: is the SAT index using the 10-60 day filtered field? Is Z filtered?

We add that all the time series are filtered with a 10-60 day bandpass filter before the regressions.

5. The composites need some measure of significance, either via comparison to the total variability, or via comparison to the inter-composite spread, or via some bootstrapping, etc. This is especially important in light of the fact that internal variability seems to play an important role in shaping extratropical ENSO teleconnections. Also, how many "samples" (days, months, seasons?) make up each composite? <https://journals.ametsoc.org/jcli/article/31/13/4991/92604/How-Well-Do-We-Know-ENSO-s-Climate-Impacts-over>

We add statistical tests based on bootstrapping to Figs. 5 and 6 and explain in the text (line 255) that "Statistical significance is assessed through a bootstrapping approach with randomly resampled (1500 times) composites of the same sample size as those shown in Fig. 5"

We add that 21 and 14 winters are used for $SVD1_{SST} > 0.5$ and $SVD1_{SST} < -0.5$, respectively. These winters are indicated with Xs and Os in Fig. 2.

OTHER POINTS

- Fig. 1: show SSV climatology?

We add a new figure (Fig. 1) to show some basic climatological features of SAT and its subseasonal variability. These features are now discussed at the beginning of the results section (lines 184-203).

- Fig. 2, 3, 4: please define abbreviations in caption

We add definitions of the abbreviations of energetics terms in each of these captions.

- L257: "an important asymmetry" - isn't this just a consequence of L252-254?

We notice this terminology can be confusing. To clarify we add (line 346): "However, an important mismatch is observed in the response of warm and cold extremes over western and southern North America (Figs. 10a-b). In these sectors, increases in the frequency of cold extremes are not matched with similar decreases in the frequency of warm extremes and *vice-versa*."

- L262: "which significantly widens the probability distribution..." I don't understand this explanation. Are you suggesting that a wider distribution mean that you "lose" extremes on one end but not the other, and if so, why?

To clarify we add the following discussion (lines 354-357): "For instance, if the winter-mean temperature is warmer, one may expect the whole probability distribution of temperature to shift towards warmer temperatures and thereby increase the likelihood of warm extremes and decrease the likelihood of cold extremes. However, if subseasonal variability is enhanced, it can contribute to increasing the frequency of cold extremes, opposing the effect of the changes in the mean"

- L286: EN and LN flipped?

Thank you very much for noticing the mistake.

References

- Barriopedro, D., and N. Calvo, 2014: On the Relationship between ENSO, Stratospheric Sudden Warmings, and Blocking. *J. Clim.*, **27**, 4704–4720, <https://doi.org/10.1175/JCLI-D-13-00770.1>.
- Bjornsson, H., and S. A. Venegas, 1997: A Manual for EOF and SVD Analyses of Climatic Data. Department of Atmospheric and Oceanic Sciences and Centre for Climate and Global Change Research: McGill University, 52 pp.
- Bretherton, C. S., C. Smith, and J. M. Wallace, 1992: An Intercomparison of Methods for Finding Coupled Patterns in Climate Data. *J. Clim.*, **5**, 541–560, [https://doi.org/10.1175/1520-0442\(1992\)005<0541:AIOMFF>2.0.CO;2](https://doi.org/10.1175/1520-0442(1992)005<0541:AIOMFF>2.0.CO;2).
- Chen, W. Y., and H. M. van den Dool, 1997: Asymmetric Impact of Tropical SST Anomalies on Atmospheric Internal Variability over the North Pacific. *J. Atmos. Sci.*, **54**, 725–740, [https://doi.org/10.1175/1520-0469\(1997\)054<0725:AIOTSA>2.0.CO;2](https://doi.org/10.1175/1520-0469(1997)054<0725:AIOTSA>2.0.CO;2).
- Renwick, J. a., and J. M. Wallace, 1996: Relationships between North Pacific Wintertime Blocking, El Niño, and the PNA Pattern. *Mon. Weather Rev.*, **124**, 2071–2076, [https://doi.org/10.1175/1520-0493\(1996\)124<2071:RBNPWB>2.0.CO;2](https://doi.org/10.1175/1520-0493(1996)124<2071:RBNPWB>2.0.CO;2).
- Soulard, N., H. Lin, and B. Yu, 2019: The changing relationship between ENSO and its extratropical response patterns. *Sci. Rep.*, **9**, <https://doi.org/10.1038/s41598-019-42922-3>.
- Straus, D. M., and J. Shukla, 2002: Does {ENSO} Force the {PNA}? *J. Clim.*, **15**, 2340–2358.
- Trenberth, K. E., G. W. Branstator, D. Karoly, a Kumar, N. C. Lau, and C. Ropelewski, 1998: Progress during TOGA in understanding and modeling global teleconnections associated with tropical sea surface temperatures. *J. Geophys. Res.*, **103**, 14291–14324, <https://doi.org/10.1029/97jc01444>.

Influence of ENSO on North American subseasonal surface air temperature variability

Patrick Martineau^{1,2}, Hisashi Nakamura^{1,2}, and Yu Kosaka^{2,4}

^{2,1}[Japan Agency for Marine-Earth Science and Technology, Yokohama, Japan](#)

5 ^{2,4}Research Center for Advanced Science and Technology, The University of Tokyo, Tokyo, Japan

~~³[Japan Agency for Marine-Earth Science and Technology, Yokohama, Japan](#)~~

Correspondence to: Patrick Martineau (pmartineau@jamstec.go.jp~~pmartineau@atmos.reast.u-tokyo.ac.jp~~)

Abstract. The wintertime influence of El Niño-Southern Oscillation (ENSO) on subseasonal variability is revisited by identifying the dominant mode of covariability between 10-60 day band-pass-filtered surface air temperature (SAT) variability over the North American continent and winter-mean sea surface temperature (SST) over the ~~North-tropical~~ Pacific ~~sector~~. We find, in agreement with previous studies, that La Niña conditions tend to enhance the subseasonal SAT variability over western North America. This modulation of subseasonal variability is achieved through interactions between subseasonal eddies and La Niña-related changes in the winter-mean circulation. Specifically, eastward-propagating quasi-stationary eddies over the North Pacific are more efficient in extracting energy from the mean flow through the baroclinic conversion ~~of energy over the North Pacific sector~~ during La Niña. Changes in the vertical structure of these ~~wave anomalies~~ ~~eddies~~ are crucial to enhance the efficiency of ~~the~~ energy conversion via amplified downgradient heat fluxes that energize subseasonal eddy thermal anomalies. The combination of increased subseasonal SAT variability and the cold winter-mean response to La Niña both contribute to enhancing the likelihood of cold extremes over western North America.

1 Introduction

20 El Niño-Southern Oscillation (ENSO), the leading mode of sea surface temperature (SST) variability over the tropical Pacific ~~sector~~, has far-reaching impacts on the atmospheric circulation in the Northern Hemisphere through the generation and propagation of a stationary Rossby wave train to the extratropics (Trenberth et al., 1998). This wave train originates in the western subtropical North Pacific, propagates initially northward, and refracts towards North America. The atmospheric response to the warm phase of ENSO (El Niño) is characterized by a strengthening of the North Pacific jet stream that also stretches further eastward, and vice versa for the cool phase (La Niña). It projects strongly on the dominant modes of atmospheric variability over the North Pacific Sector (Alexander et al., 2002; Horel and Wallace, 1981), including the Pacific North American (PNA) pattern (Wallace and Gutzler, 1981), under the feedback forcing from the modulated stormtrack activity (Lau, 1997). ~~The atmospheric response to the warm phase of ENSO (El Niño) is characterized by a strengthening of the North Pacific jet stream that also stretches further eastward, and vice versa for the cool phase (La Niña).~~

30 In addition to its effect on the extratropical winter-mean atmospheric circulation, ENSO also influences intraseasonal variability. Nakamura (1996) identified a mode of year-to-year covariability between the winter-mean tropospheric circulation and subseasonal variability over the North Pacific sector. This mode is characterized by extratropical winter-mean circulation anomalies that strongly resemble the atmospheric response to ENSO and the PNA pattern. More specifically, winter-mean anticyclonic anomalies that are associated with the weakened surface Aleutian Low ~~and with the~~
35 ~~negative phase of the PNA~~ tend to be accompanied by an increase of subseasonal variability over the North Pacific. The associated SST anomalies are characterized by warm anomalies in the central North Pacific, indicative of a possible connection with La Niña. Similarly, Renwick and Wallace (1996) noted an increase of subseasonal variability over the North Pacific in La Niña winters, ~~and~~ (Lin and Derome, (1997) documented an enhancement of subseasonal variability in negative PNA years. Since then, many studies have confirmed ENSO's modulations of subseasonal variability (Chen and Dool, 1999;
40 Chen and van den Dool, 1997; Compo et al., 2001; Tam and Lau, 2005). This ENSO influence ~~of ENSO~~ on subseasonal variability not only affects the mid-tropospheric flow as shown ~~in~~ by many of these studies but also has a clear impact on surface air temperature (SAT), potentially modulating the occurrence of weather extremes. In fact, Smith and Sardeshmukh (2000) have shown that the intraseasonal temperature variance is enhanced over the North American West Coast ~~during~~
under La Niña conditions.

45 This ENSO influence on intraseasonal variability may be achieved in part through modulation of the frequency of blocking events
~~In agreement with ENSO's modulation of subseasonal variability, blocking events~~, which are prominent and persistent atmospheric circulation anomalies that exert an important influence on SAT variability (Buehler et al., 2011; Martineau et al., 2017; Pfahl and Wernli, 2012; Rex, 1950). For instance, blocking events have been associated with some extreme cold spells in winter (Brunner et al., 2018; Buehler et al., 2011; Cattiaux et al., 2010; Sillmann et al., 2011). ~~They were also shown to occur preferentially for a specific phase of ENSO.~~ Several studies have noted an enhancement of blocking activity during La Niña (Barriopedro and Calvo, 2014; Chen and van den Dool, 1997; Renwick and Wallace, 1996). ~~while~~ Others, however, have ~~rather~~ noted a shift in the preferred location of blocking (Mullen, 1989) or even a decrease in blocking occurrence
55 differences in the definition of blocking events, which are sometimes defined as a reversal of the zonal flow in the mid-latitudes and other times as prominent anticyclonic anomalies. The studies that have defined blocking events as prominent anomalies have reported an increase in the frequency of blocking during La Niña (Barriopedro and Calvo, 2014; Chen and van den Dool, 1997; Renwick and Wallace, 1996), which is in agreement with the aforementioned changes in intraseasonal variability. Considering the link between blocking and weather extremes, this suggests a potential increase in the frequency
60 of extreme cold episodes on subseasonal time scales during La Niña.

Several mechanisms have been proposed to explain ENSO's influence on extratropical subseasonal variability. Tam and Lau (2005) suggested that changes in the tropical source of quasi-stationary Rossby eddies, resulting from ENSO's influence on MJO activity, and changes in the propagation of these wave trains under the modulated refractive properties of the mid-

latitude westerlies by ENSO were among the plausible causes. Changes in barotropic energy conversion, i.e., the direct transfer of kinetic energy between the climatological jet stream and subseasonal eddies, forced by ENSO variability, and changes in the feedback forcing by high-frequency eddies due to shifts in the preferred location of the storm track were also proposed as possible mechanisms (Chen and Dool, 1999; Chen and van den Dool, 1997). High-frequency eddy feedback and interactions between low-frequency variability and the mean flow were also shown to contribute ~~strongly~~ to the enhancement of subseasonal variability during the negative phase of the PNA (Lin and Derome, 1997) and thus may also be effective during La Niña winters whose extratropical response shares similarities with the PNA as discussed earlier.

Some of these Pprevious studies ~~often~~ assumed that the structures of atmospheric circulation anomalies associated with subseasonal variability is ~~are~~ predominantly equivalent barotropic, i.e., with ~~structures that have~~ slight or even no vertical tilts, and have consequently focused only on barotropic processes alone ~~to explain ENSO's modulation of subseasonal variability;~~ and thus the ~~The role of~~ dynamical processes linked to the vertical dependence of ~~their~~ these subseasonal structures, or baroclinicity, in this modulation remain poorly understood. Tam and Lau (2005) nevertheless noted a vertical dependence of the structure of the quasi-stationary waves associated with subseasonal variability over the North Pacific. They have discussed the possibility, without evaluating it, ~~however~~ though, that baroclinic processes may play a role. Recently, Sung et al. (2019) found that the recent decadal shift of the Tropical Pacific into La Niña-like condition has ~~ve~~ modified baroclinic energy conversion into the North Pacific Oscillation (NPO; ~~Barnston and Livezey, 1987; Linkin and Nigam, 2008; Wallace and Gutzler, 1981~~), leading to enhanced winter monthly-mean temperature extremes over North America. It is thus plausible to hypothesize that ENSO's influence on subseasonal variability may result, at least in part, from the modulated baroclinicity of the seasonal-mean circulation in the extratropics and the vertical structure of eddies. This hypothesis is reasonable since subseasonal variability does exhibit vertically-tilting structures (Blackmon et al., 1979; Cai et al., 2007; Dole, 1986; Taguchi and Asai, 1987) which play an important role in energizing these eddies (Cai et al., 2007; Sheng and Derome, 1991; Tanaka et al., 2016).

The key goal of this work is thus to assess the role of baroclinic processes in ENSO's modulations of subseasonal variability over the North Pacific sector. As a first step, we identify the dominant mode of covariability between tropical North Pacific SST anomalies and subseasonal SAT variability affecting the ~~eastern Pacific sector and~~ North American continent through a singular value decomposition analysis. By focusing on surface variability instead of mid-tropospheric variability, this study aims to better understand the dynamical processes that regulate persistent sub-seasonal SAT anomalies that have large socio-economic impacts. Without surprise, ENSO-like SST variability emerges from this analysis as the dominant influence on North American subseasonal SAT variability. In agreement with Smith and Sardeshmukh (2000), La Niña conditions tend to enhance the variability over Western North America.

As a second step, we evaluate how changes in the extratropical winter-mean circulation forced by ENSO modulate subseasonal eddy energy. We compare ~~The~~ the contributions ~~roles~~ of ~~between~~ baroclinic and barotropic energy conversions from the winter-mean flow to atmospheric circulation anomalies ~~on subseasonal time scales, hereafter referred to as~~ subseasonal eddies, ~~are assessed~~. In addition, we ~~also~~ assess the roles of high-frequency eddy feedback and diabatic

processes in the energetics. From this analysis, baroclinic energy conversion, which is tied to the vertically-tilting structure of subseasonal circulation anomalies, stands out as the primary source of energy by which ENSO modulates subseasonal variability.

~~Concerning ENSO's influence on the frequency of warm and cold temperature extremes, we find that the impacts of ENSO on both winter mean SAT and subseasonal SAT variability contribute to the enhanced likelihood of cold extremes over North America during La Niña.~~

2 Methodology

2.1 Data

This study uses [6-hourly](#) reanalysis data [of the global atmosphere](#) from the Japan Meteorological Agency 55-year Reanalysis (JRA-55, Kobayashi et al. 2015) from 1958 to 2016. Variables analysed include the three-dimensional wind field (u, v, ω), temperature (T), geopotential height (Z), parameterized diabatic heating (Q) and temperature 2 meters above the surface (SAT). SST is obtained from the HadISST dataset (Rayner et al., 2003).

2.2 Singular value decomposition analysis

~~One approach to investigating the influence of ENSO on subseasonal SAT variability is to start from classic ENSO indices (see the next section). The individual indices, however, many indices are associated with ENSO (see next section) and each represents a different “flavours” of ENSO which that may have exert a distinct influence impacts on North-American subseasonal SAT variability. Instead of repeating our analysis for all these indices, we identify, via singular value decomposition (SVD) analysis (Bjornsson and Venegas, 1997; Bretherton et al., 1992), the a particular “flavour” of tropical Pacific SST variability that is optimally related to subseasonal SAT variability over North America. Identifying this optimal influence is not only important to better predict SAT variability from SST anomalies but also contributes to improving the clarity of the rest of our analyses by focusing on the strongest statistical connection.~~

~~Singular value decomposition~~ Here, (SVD) analysis (Bjornsson and Venegas, 1997; Bretherton et al., 1992) is used to identify the dominant mode of covariability between winter-mean (December-January-February) SST over the [tropical Pacific sector](#) ([20°S-60°N](#), [120°E-80°W](#)) and subseasonal SAT variability (SSV; [defined as the](#) local standard deviation of 10-60 day bandpass-filtered [6-hourly SAT](#) ~~overduring December-January-February~~ [the winter season](#)) over the Eastern North Pacific and North-American sectors ([20°N-60°N](#), [140°W-60°W](#)). The sectors used for the two variables are illustrated in Fig. [1-2](#) with dashed rectangles. Results are not sensitive to small variations in these sectors. After obtaining the SST and SSV patterns from the SVD analysis, time series expressing their time evolution (SVD_{1SST} and SVD_{1SSV}) are obtained by projecting the original SST and SSV anomaly fields onto these patterns. The SST and SSV patterns shown in

130 this study are not the original patterns directly obtained from the SVD but rather heterogeneous regressions, i.e., SSV regressed onto SVD_{1SST} and SST regressed onto SVD_{1SSV}. The heterogeneous patterns are similar to the original homogeneous patterns, indicating strong coupling between the two fields. The statistical significance of the regressed heterogeneous patterns is assessed with a *t*-test for the correlation coefficient at the 95% confidence level.

2.3 ENSO indices

135 The SVD_{1SST} time series is compared to classical ENSO indices to identify the index that is optimally related to North American SAT variability. The ENSO indices are obtained by averaging SST anomalies over various sectors followed by a normalization of each index. The sectors are [10°S-0°, 90°W-80°W] for Niño1+2, [5°S-5°N, 150°W-90°W] for Niño3, [5°S-5°N, 170°W-120°W] for Niño3.4, and [5°S-5°N, 160°E-150°W] for Niño4 (Bamston et al., 1997).

2.4 Energetics of subseasonal eddies

140 Atmospheric energetics (Lorenz, 1955; Oort, 1964) are used to assess how ENSO modulates the sources of energy sustaining circulation anomalies ~~that~~ produce subseasonal SAT variability (or SSV). Energies and their conversion/generation terms are integrated vertically from the surface to 100 hPa for subseasonal variability that has been extracted by applying a 10-60 day bandpass filter to the 6-hourly data (denoted with primes in the following equations). The basic state, denoted with overbars, is defined as the winter-mean (DJF) fields for individual years, ~~which~~ that include seasonal-mean fluctuations related to ENSO variability.

145 The eddy available potential energy (EAPE), is defined as

$$EAPE = \gamma^{-1} \frac{T'^2}{2}, \quad (1)$$

where γ is a stability parameter defined as

$$\gamma = \frac{p}{R} \left(\frac{R\hat{T}}{C_p p} - \frac{\partial \hat{T}}{\partial p} \right). \quad (2)$$

150 Here R is the gas constant for dry air (287 J K⁻¹ kg⁻¹) and C_p is the specific heat at constant pressure (1004 J K⁻¹ kg⁻¹). The stability parameter is here based on temperature averaged over the Northern Hemisphere (denoted by the hat operator). The EAPE is proportional to temperature variance when averaged over a season and receives a strong contribution from the lower troposphere where subseasonal temperature anomalies are strongest (not shown).

Several sources of EAPE are considered. The first is baroclinic energy conversion (CP):

$$CP = -\gamma^{-1} \left(u'T' \frac{\partial \hat{T}}{\partial x} + v'T' \frac{\partial \hat{T}}{\partial y} \right). \quad (3)$$

155 It describes how available potential energy is transferred from the winter-mean flow to subseasonal eddies, which is achieved through downgradient eddy heat fluxes. We also consider feedback forcing on EAPE by high-frequency eddies (~~double primes~~; Tanaka et al., 2016) which are that have been extracted with a 10-day high-pass filter (double primes):

$$CP_{HF} = -\gamma^{-1}T' \left(\frac{\partial(u''T'')'}{\partial x} + \frac{\partial(v''T'')'}{\partial y} \right). \quad (4)$$

CP_{HF} describes how high-frequency eddy heat fluxes act to reinforce or dampen subseasonal temperature anomalies.

160 Diabatic processes can also play a role in the maintenance or dissipation of EAPE. It is evaluated here with

$$CQ = \gamma^{-1} \frac{Q'T'}{c_p}, \quad (5)$$

where Q is the heating rate. Diabatic processes and parameterized vertical heat diffusion, which are provided by JRA-55, are all included in Q .

We also investigate ENSO's modulation of eddy kinetic energy (EKE), defined as

$$165 \text{ EKE} = \frac{u'^2 + v'^2}{2}, \quad (6)$$

where u' and v' are wind anomalies associated with subseasonal eddies. The sources of EKE considered here include barotropic energy conversion (CK) from the seasonal-mean flow to subseasonal eddies (Oort, 1964; Simmons et al., 1983)

$$CK = \frac{v'^2 - u'^2}{2} \left(\frac{\partial \bar{u}}{\partial x} - \frac{\partial \bar{v}}{\partial y} \right) - u'v' \left(\frac{\partial \bar{u}}{\partial y} + \frac{\partial \bar{v}}{\partial x} \right), \quad (7)$$

the feedback forcing from high-frequency eddies (CK_{HF} ; Tanaka et al. (2016)) defined as

$$170 \text{ CK}_{HF} = -u' \left(\frac{\partial(u''u'')'}{\partial x} + \frac{\partial(u''v'')'}{\partial y} \right) - v' \left(\frac{\partial(u''v'')'}{\partial x} + \frac{\partial(v''v'')'}{\partial y} \right), \quad (8)$$

and transfers of energy between EAPE and EKE

$$CPK = -CKP = -\frac{R\omega'T'}{p}, \quad (9)$$

which is achieved through vertical motion. Here a positive CPK denotes a transfer from EAPE to EKE and *vice-versa*.

The spatial redistribution of energy by mean flow related fluxes of energy ($-\nabla \cdot \bar{\mathbf{u}}(EAPE + EKE)$) and pressure work ($-\nabla \cdot (\mathbf{u}'\Phi')$) are not assessed in this work since they have no net contribution to the modulation of subseasonal eddy energy after integrated over a large domain.

We here evaluate the efficiency of energy conversion by normalizing dividing the conversion terms by the total eddy energy (EAPE + EKE) for each winter. For instance, the efficiency of CP may be evaluated as CP^{eff} , which is defined as

$$CP^{\text{eff}} = \frac{\langle CP \rangle}{\langle EAPE + EKE \rangle}, \quad (10)$$

180 where the angle brackets denote an average over the months of DJF, a vertical integral from the surface to 100 hPa and integration over the entire North Pacific (10° - 87.5° N, 120° E- 55° W).

3 Results

3.1 A preliminary survey of surface air temperature variability

185 Before investigating modes of covariability, it is useful to look at basic climatological properties of SAT variability. The winter-mean SAT climatology is characterized by stronger SAT gradients over North America in comparison to the surrounding ocean bodies (Fig. 1a). They are especially large in the mid-latitudes over the eastern portion of North America (Fig. 1a) but also at high-latitudes on the western coast of the conterminous United States, Canada, and Alaska. The Northwest-Southeast-tilted isotherms reflect the temperature contrast between the warmer North Pacific waters and the colder land surfaces. SSV (Fig. 1b), as defined in this study, is largest over a band stretching from the Bering Strait, Alaska, and Western Canada. In contrast, more moderate SSV is found over Northern Central US, Eastern Canada, and part of Greenland. Overall, SSV is markedly larger over land surfaces.

190 The climatological SSV is then contrasted to climatological high-frequency SAT variability (Fig. 1c), which is associated with the passage of transient synoptic-scale systems such as cyclones and anticyclones. High frequency variability and is has been extracted here by using a 2-8 day band-pass filter. One notices the signatures of the storm tracks in high-frequency SAT variability over the North Pacific Ocean and the western boundary of the North Atlantic Ocean (Fig. 1e). Due to the damping of temperature anomalies by air/sea heat exchanges, the maximum high-frequency variability is found over land, and is especially specifically large over Eastern Canada. In that sector region, high-frequency variability and SSV have similar magnitudes, but elsewhere SSV is markedly dominant. This illustrates that SAT variability at the subseasonal time scale constitutes an important part of total intraseasonal SAT fluctuations over the North American continent.

200 The interannual variability of subseasonal SAT variability, calculated as the standard deviation of SSV, is generally large where the climatology of SSV is also large (comparing Figs. 1b and 1d) with maxima over the Bering Strait, Western Canada, Northeastern Canada, and Southwestern Greenland. It corresponds to fluctuations of about 20-30% of the climatology depending on the sector-specific locations.

205 3.1.2 ENSO's influence on North American surface temperature variability

The dominant mode of covariability (SVD1) between SSV and SST (Fig. 2), identified through the SVD analysis described in section 2.2, explains about 70.56% of the total squared covariance between the two fields (Fig. 21). It is characterized by a significant increase of SSV over the western U.S., Canada, Alaska, and Eastern Siberia, (up to ~10% of the climatology) whose magnitude is up to ~10% of the SSV climatology (see Fig. 1b). The variability represented by this pattern explains up to about 10% of the total local interannual SSV variability over the western U.S., Canada, Alaska, and Eastern Siberia. This enhancement of SSV in association is associated with prominent cold SST anomalies over the Eastern Equatorial Pacific and weaker warm anomalies over the Western Equatorial Pacific. These significant SST anomalies are strongly reminiscent of the cold phase of ENSO, La Niña. Indeed, the time series representing the temporal variability of this pattern (SVD1_{SST}, Fig.

215 [2+c](#)) is strongly anticorrelated to all the four Niño indices (Table 1). SVD1_{SST} is most strongly anticorrelated to the Niño 3 and Niño 3.4 indices, indicating a dominant link between Eastern Equatorial Pacific variability and SSV over North America. The anti-correlations between SVD1_{SSV} and two other Niño indices are also strong and statistically significant. Meanwhile, the correlation between SVD1_{SST} and SVD1_{SSV} is significant but rather modest, which suggests that factors other than ENSO, such as internal atmospheric variability or other teleconnections, may also affect subseasonal SAT variability in a similar manner. Such a possibility is briefly explored later.

220 The regression ~~map-pattern~~ of winter-mean 500-hPa Z (Z500) onto the SVD1_{SSV} index (Fig. [2+b](#)) resembles La Niña's impact on the extratropical atmospheric circulation that [has](#) features [similar to](#) the negative phase of the PNA. [We note, however, that it is more similar to the extratropical response forced by ENSO than the internally-generated PNA.](#) (Straus and Shukla, 2002). Specifically, cyclonic anomalies are found over the Western subtropical Pacific and Canada, ~~and~~ [while](#) anticyclonic anomalies are over the midlatitude North Pacific north of 40°N. These anomalies constitute a Rossby wave train refracting around the Eastern North Pacific, as suggested by the wave-activity flux (Takaya and Nakamura, 2001). This anomaly pattern ~~represents~~ [accompanies](#) the weakened and more diffluent North Pacific [westerly](#) jet ~~than in comparison to the climatology~~ (not shown).

3.3.2 Processes through which ENSO affects subseasonal eddy activity

230 In this section, we evaluate ENSO's influence on subseasonal eddy activity by assessing ENSO's modulations of various sources/sinks of eddy energy. [The rationale is that SSV is produced by weather systems \(or eddies\) that have deep structures within the troposphere and thus a better understanding of interannual fluctuations of SSV can be acquired through investigating year-to-year changes in processes that energize these eddies.](#) For this analysis, all components of the winter-mean energy budget for subseasonal eddies described in Sect. 2.4 are regressed onto SVD1_{SST}. As a reminder, this index is strongly anticorrelated to the Niño 3.4 index. A positive SVD1_{SST} index is, therefore, representative of ENSO's cold phase (La Niña), and all the regression patterns show the linear response to ENSO featuring its cold phase. Note that we have also carried out a composite analysis for El Niño and La Niña winters separately and found salient features to be mostly linear.

240 Figures ~~2a~~[3a](#)-b show anomalies of EAPE and EKE corresponding to a unit standard deviation of the SVD1_{SST} index. Both EAPE and EKE tend to overall increase ~~during~~ [under](#) La Niña conditions, ~~and~~ [the increased EAPE](#) ~~former of which~~ is consistent with the enhanced SSV of SAT over the landmasses. Whereas the EAPE signal is mostly concentrated over landmasses north of the Pacific Ocean and over North America, the EKE signal is particularly large over the subpolar North Pacific ~~sector~~. Integrated over the whole North Pacific (Fig. [3d](#)), the energy increase is roughly equipartitioned between EAPE and EKE, but slightly larger for the latter.

245 Next, we examine the corresponding changes in the conversion of energy from the winter-mean flow to subseasonal eddies through the baroclinic (CP) and barotropic (CK) conversions. A large increase in CP is observed [extensively](#) over the subpolar North Pacific with its maximum over the Gulf of Alaska, which contributes to an increase of CP^{eff} over the entire North Pacific (Fig. [43](#)). [The large CP increase occurs where subseasonal eddies exhibit baroclinic structure, especially in](#)

the lower troposphere, with climatologically positive correlation between v' and T' (Fig. 6). Like CP, CK also tends to increase over the mid-latitude North Pacific (Fig. 23d), but overall, the contribution of CK is weaker-smaller than that of CP (Fig. 43).

250 As per their definition, CP and CK depend on both the winter-mean flow configuration and eddy properties. To assess their relative importance, we compute composite differences between years-winters when the normalized SVD1_{SST} is above 0.5 or below -0.5, as the 21 and 14 winters indicated with Xs crosses and Os open circles, respectively, in Fig. 2c. The composite differences in which both the eddy properties and basic-state properties are allowed to vary from year to year (Figs. 54e-f) are contrasted to the corresponding composites in which the basic-state properties (Figs. 54a-b) or eddy properties (Figs. 54c-d) are set-fixed to their climatologies from 1979 to 2015. Statistical significance is assessed through a bootstrapping approach with randomly resampled (1500 times) composites of the same sample size as those shown in Fig. 5. The comparison reveals that year-to-year changes in eddy properties are essential to explain the enhanced CP over the Pacific sector (comparing Fig. 54a to Fig. 54e). We note that although the total composite difference of CP and the one using constant eddy properties are both significant over the Northwestern Pacific (Figs. 5c,e), the significance is somewhat 260 reduced for the composite difference with the constant basic state (Fig. 5a) is less so. We suspect this may be due to a cancellation of ENSO-unrelated noise when fluctuations in both eddy and winter-mean properties are considered, which contributes to increasing the statistical significance. Over the sectors-domain of enhanced CP, we find evidence of-for a stronger positive correlation between v' and T' (Fig. 65) throughout the depth of the troposphere, which indicates that the structure of subseasonal eddies is more adequate in La Niña winters to extract energy from the meridional thermal gradient of the background state-for their baroclinic growth from the meridional thermal gradient associated with the Pacific jet. The increased CP is also found to arise from We also find that the tendency for the climatologically positive and negative correlations between u' and T' are-to be enhanced over Alaska and the Okhotsk Sea, where the zonal temperature gradients are climatologically positive and negative, respectively, which also contribute to the increased CP. Concerning CK, Meanwhile, the enhanced barotropic conversion CK over Alaska results from changes in eddy properties, while the 265 changes over the Western North Pacific appear to result from a combination of changes in both eddy and winter-mean flow properties (Fig. 54 right).

The contributions of CP and CK are found to be much larger than the feedback forcing by high-frequency transients (CP_{HF} and CK_{HF}), which are weaker and contribute minimally to the changes in the energetics (Figs. 32e-f and 43). Similarly, diabatic feedback (CQ) has a negligible contribution.

275 Finally, we also investigate the transfer (CPK) between EAPE and EKE. We find that CPK is enhanced over a broad domain stretching northeastward from the western subtropical North Pacific to Alaska (Fig. 32h). This sector-domain is collocated with the region of enhanced CP (Fig. 32c), which indicates that an important portion of the gains in EAPE through CP is transferred to EKE in-situ. This transfer is small compared to CP, but about half of CK and thus relevant to the observed increase in EKE. Changes in the correlation between ω' and T' are overall not well organized (Fig. 56) which suggests that

280 changes in CPK are mostly due to changes in the ~~magnitudes~~ amplitude of the ~~eddy terms~~ eddies' ~~their~~ structures.

3.4.3 Changes in propagation and structure of subseasonal eddies

In this section, we assess ENSO's influence on the propagation of wave activity ~~and~~ in relation to the structure of subseasonal eddies. Subseasonal eddy propagation is first assessed by using the wave activity flux for stationary Rossby waves (Takaya and Nakamura, 1997, 2001) computed from 10-60 day band-pass filtered 6-hourly Z500. It is computed for each time step after filtering and then averaged over the winter months (DJF) before being regressed onto SVD1_{SST}. The flux, which is climatologically eastward (not shown) reflecting eastward group velocity of stationary Rossby waves, tends to be enhanced during La Niña winters (Fig. 76). The enhanced eastward flux ~~is observed~~ maximizes over the subpolar North Pacific, where CP is enhanced, and over western North America, where SSV also increases noticeably. The eastward wave-activity flux is also enhanced just east of the region of enhanced CK over the subtropical North Pacific.

Next, we ~~evaluate~~ perform through lag-regression analysis to identify the typical structure of ~~the~~ quasi-stationary eddies that are associated with subseasonal SAT variability over western North America (Fig. 87). The analysis is carried out with reference subseasonal SAT time series over Alaska and Colorado. These locations are chosen because SVD1 has a large impact on SSV over these sectors (Fig. 2). ~~These~~ reference time series are normalized so that the regressed patterns represent circulation anomalies associated with typical SAT variability. All the time series are have been filtered exposed to with a 10-60 day bandpass filter before evaluating the regressions. The instantaneous regression map corresponding to Alaska SAT variability shows a clear wave train propagating eastward (Fig. 87e). The wave train is mostly stationary with little phase propagation from lag -3 (day) to lag 0 (Figs. 87c,e). At all lags, positive correlations are observed over the subtropical North western Pacific, suggesting a potential subtropical origin to this wave train. Precursors are also observed over Russia at lag -6 (Fig. 87a) as well as lags -9 and -12 (not shown), indicating that this wave train may also originate from the extratropics. The same instantaneous regression performed for a reference SAT index over Colorado also reveals an eastward-propagating wave train (Fig. 87f). Through the lag regression analysis, the origin of this wave train can be traced back in part to the subpolar North western Pacific and the subtropical central Pacific (Figs. 87b,d). In this case, the phase of the wave train is seen to move slowly eastward. As illustrated in Fig. 8, atmospheric circulation patterns associated with localized SAT variability are quite sensitive to the reference location. These patterns share similar features, such as their spatial scale and meandering, with the circulation anomalies associated with the leading modes of SAT variability (Lin, 2015). The exact location of their cyclonic and anticyclonic centres of action are, however, not the same. They may correspond to modes of lesser importance or combinations of the leading modes. Other reference locations over North America were assessed and revealed different circulation anomalies (not shown).

310 ~~Both~~ The two quasi-stationary wave ~~structures~~ trains revealed by the regression analysis propagate through the North Pacific sector where CP and CK are enhanced. Significant differences in the amplitude of these wave trains are observed between the two phases of SVD1_{SST}. Differences in the Z500 regression pattern tend to be positive where the Z500 anomalies are

typically positive and *vice-versa*, which indicates an overall intensification of ~~the amplitude of the wave patterns~~ trains ~~during~~ under La Niña conditions. It is consistent with the enhanced eddy energy and wave activity fluxes discussed previously.

To understand better how quasi-stationary eddies ~~more efficiently~~ can extract energy more efficiently from the winter-mean flow through heat fluxes ~~during~~ in La Niña winters than in El Niño winters, we also ~~analyse through~~ construct one-point regression maps to highlight the vertical structure of these eddies separately for those two types of winters (Fig. 98). Their structure is evaluated over the North Pacific, where the enhanced positive correlation between v' and T' (Fig. 65) hints to important zonal structural changes that lead to a substantial modulation of CP (Fig. 3c). For a robust illustration of the structure of eddies over that sector, it is preferable to use a local reference grid point in this analysis (as indicated with a green circle in Figs. 3c and 6). Eddy structures constructed from remote reference SAT time series over Alaska and Colorado (Fig. 8) do exhibit signals over the North Pacific, but the correlations are substantially weaker which indicates a low signal to noise ratio. For a robust illustration of the structure of eddies, it for this analysis is in the SAT regions but the substantially. Indeed, As expected from the enhanced CP and correlation between v' and T' , the westward tilt of the geopotential height structure anomalies is enhanced when $SVD1_{SST} > 1$ (Figs. 9a-b), which is consistent with the enhanced $v'-T'$ correlation. Whereas the westward tilt is found throughout the depth of the troposphere when $SVD1_{SST} > 1$, it is somewhat weaker and limited to the lower troposphere when $SVD1_{SST} < -1$. Also Correspondingly, the geopotential height anomalies are slightly out of phase with temperature anomalies at all levels even above the 700-hPa level when $SVD1_{SST} > 1$, whereas they are almost out of phase only below in phase between 700 hPa and 500 hPa when $SVD1_{SST} < -1$. The net meridional heat fluxes associated with these structures (Figs. 9c, d) are obviously overall larger for $SVD1_{SST} > 1$ -due to an marked enhancement (approximate doubling) of poleward heat transport to the west of the reference longitude, which cannot be offset completely by a slight increase in while the southward transport to the east is increased to a lesser extent. -These changes in the vertical structure of subseasonal eddies and the associated heat fluxes, manifested also as the enhanced positive $v'-T'$ correlation (Fig. 65), allow to give rise to a more efficient downgradient heat transport during La Niña winters ($SVD1_{SST} > 1$), thus leading to a more efficient extraction of energy from the winter-mean flow through baroclinic conversion (Fig. 34).

3.5.4 Impact on extreme temperature events

The impact of $SVD1_{SST}$ /ENSO variability on the occurrence of persistent weather extremes is now investigated. Cold (warm) extreme days are defined as the days when the 10-day lowpass-filtered SAT anomaly falls below (rises above) the 5th (95th) percentiles at each grid point over the 58 winters. Their frequency, calculated as the percentage of winter days each year, is then regressed onto the $SVD1_{SST}$ time series. The spatial patterns of changes in the frequency of weather extremes (Figs. 109a-b) are similar to the winter-mean SAT response (Fig. 109c) with an enhanced frequency of cold extremes over the regions that are colder than normal and *vice-versa*. Generally, the corresponding relationship holds also between warm extremes and winter-mean SAT. This indicates that the winter-mean response to ENSO variability plays a major role in setting the frequency of extremes, through shifts in the probability distributions of temperature.

However, an important ~~asymmetry-mismatch~~ is observed in the response of warm and cold extremes over western and southern North America (Figs. 9-10a-b). In these sectors, increases in the frequency of cold extremes are not matched with similar decreases in the frequency of warm extremes and vice-versa. In Alaska and western Canada, for example, colder winter-mean SAT under the La Niña conditions accompany an increase in the frequency of cold extremes, while the corresponding changes in the frequency of warm extremes are rather small and insignificant over land. Likewise, in the southern U.S., the anomalous winter-mean warmth increases the frequency of warm extremes but the frequency changes of cold extremes are small. These ~~asymmetries-mismatches~~ arise from the enhanced subseasonal variability (Fig. 109d), which significantly widens the probability distribution of SAT over these ~~sectors~~ regions. For instance, if the winter-mean temperature is warmer, one may expect the whole probability distribution of temperature to shift towards warmer temperatures, and as a result, thereby increase the likelihood of warm extremes and decrease the likelihood of cold extremes. However, if subseasonal variability is enhanced, it can contribute to increasing the frequency of cold extremes, opposing the effect of the shift changes in the mean. Changes in skewness also contribute to altering the frequency of warm and cold extremes over some sectors, but their contribution is overall ~~spatially~~ less organized spatially and also statistically insignificant (not shown).

3.6.5 Modulation of subseasonal SAT variability unrelated to ENSO

As mentioned earlier, SVD1_{SSV} is ~~moderately~~ rather moderately ~~to~~ with SVD1_{SST} and Niño indices (Table 1), which suggests that a substantial fraction of year-to-year variations in SSV over the North American West Coast may arise from internal atmospheric variability. The processes responsible for this variability are briefly assessed. The component of SVD1_{SSV} that is uncorrelated with SVD1_{SST} (SVD1_{RSSV}) is first identified as the residual of the linear regression between the two indices. By regressing SSV onto the index (Fig. 110a), we find an amplification of SSV whose spatial structure is similar to the one previously identified (Fig. 24a) and whose intensity is notably augmented over North America (up to ~15% of the climatology (Fig. 1b) and 50% of total interannual variability explained). The correlations of SVD1_{RSSV} with the ENSO indices are indeed quite weak ~~overall~~ and overall insignificant ~~except for the Niño 4 index~~ (Table 2). ~~Consistently,~~ ~~†~~ The corresponding grid-by-grid correlation with SST is significant only in the central Equatorial Pacific (Fig. 110b). Stronger SST anomalies are ~~however~~ nevertheless found in the midlatitude North Pacific with a pattern somewhat reminiscent of the North Pacific Gyre Oscillation (NPGO) (Di Lorenzo et al., 2008). While the winter-mean circulation pattern associated with SVD1_{RSSV} (Fig. 110b) shares some similarities with the negative phase of the PNA, it is also similar to the negative phase of the NPO. In fact, Di Lorenzo et al. (2008) indicated that the NPGO is driven by wind stress curl anomalies associated with the NPO. We argue that SVD1_{RSSV} ~~related~~ associated variability is related to the internal variability of the eddy-driven jet over the North Pacific. The feedback of NPGO-like SST anomalies onto the atmospheric anomalies in Fig. 110b needs to be addressed in future studies. Like SVD1, SVD1_{RSSV} enhances the efficiency of the baroclinic conversion of energy from the winter-mean flow over the North Pacific and the propagation of quasi-stationary waves towards North America (not shown), which acts to enhance SAT variability over the continent.

4 Summary

380 By identifying the dominant mode of interannual covariability between winter-mean tropical SST and subseasonal SAT variability, this study confirms the prominent role of ENSO in modulating the SAT variability over North America. El Niño and La Niña tend to ~~enhance~~reduce and ~~reduce~~enhance SAT variability, respectively (Smith and Sardeshmukh, 2000). Among the classical ENSO indices, the Niño 3 and Niño 3.4 indices are most closely ~~associated~~correlated with the mode of variability identified in this work.

385 Energetics of subseasonal atmospheric eddies reveals that La Niña is not only accompanied by an augmentation of EKE (Chen and Dool, 1999) but also by an increase of EAPE over the North Pacific sector, ~~as~~which is consistent with the rise of subseasonal SAT variability. In fact, the ENSO's modulation of baroclinic energy conversion is found more important than the barotropic processes emphasized in previous studies (Chen and van den Dool, 1997; Tam and Lau, 2005). The baroclinic energy conversion to subseasonal eddies is achieved through ~~eddy~~their heat fluxes that are downgradient of the winter-mean temperature ~~associate~~wd with the Pacific jet ~~climatology~~. Alternatively, this conversion can be interpreted as the anomalous thermal advection by subseasonal eddies acting on the climatological temperature gradient in such a way that it reinforces eddy temperature anomalies. In contrast to the baroclinic energy conversion, the net feedback forcing ~~of~~from high-frequency eddies migrating along the Pacific stormtrack, which was suggested as an important process (Chen and Dool, 1999; Chen and van den Dool, 1997), is much smaller. It is explained by the fact that previous studies have only assessed the
390 budget of kinetic energy in the upper troposphere, which overemphasizes the feedback ~~of~~from high-frequency eddies on the kinetic energy (Lau and Nath, 1991) and overlooks the cancellation between high-frequency eddy feedbacks onto the eddy available potential energy and eddy kinetic energy (Tanaka et al., 2016).

Although lag-regression maps suggest that the subseasonal eddies affecting SAT over North America originate in part from the Tropics, the modulation of subseasonal eddy energetics by ENSO is dominated by modulated baroclinic energy conversions in the mid to high latitudes. This suggests that ENSO's influence is not a simple manifestation of modulated tropical sources of subseasonal variability, as suggested by Tam and Lau (2005). This conclusion is also supported by the absence of significant changes in EAPE or EKE in the ~~Tropics~~Western Tropical Pacific and the fact that the modulation of energy sources by diabatic processes is comparatively very small. It is more likely that subseasonal wave trains forced by normal levels of tropical convective activity can extract more energy from the winter-mean ~~westerlies~~Pacific jet under La
405 Niña conditions as they propagate through the mid and high latitudes ~~under La Niña conditions~~.

We have further revealed that changes in the properties of subseasonal eddies are essential for the enhancement of baroclinic energy conversion during La Niña winters. In comparison, ENSO-related changes in winter-mean ~~background~~ flow properties have a rather modest direct impact on the energetics. The background flow properties, however, may have an indirect impact through their influence on the propagation and structure of subseasonal eddies. Over the midlatitude North
410 Pacific, subseasonal anomalies in eddy velocity and temperature ~~anomalies~~ are overall better correlated during La Niña winters, which translates into larger downgradient eddy heat fluxes and consequently into more efficient baroclinic energy

conversion [for their growth and maintenance](#). The enhanced correlation results from a more pronounced vertical tilt of eddies and the more out-of-phase relationship of ~~the maxima of eddy~~ geopotential height and temperature [anomalies](#) throughout the depth of the troposphere.

415 Our analysis thus suggests that, during La Niña [winters](#), the ~~growth activity~~ of subseasonal eddies is enhanced over the North Pacific as they propagate [eastward](#) towards North America. Once they reach the North American coast, these eddies have strong signatures in lower-tropospheric temperatures; due to the reduced near-surface damping of temperature anomalies over land in comparison to over the ocean, thereby enhancing SAT variability. This enhanced [SAT](#) variability, combined with cold winter-mean ~~temperature~~ anomalies during La Niña, contributes to enhancing the likelihood of
420 persistent cold extremes, especially over western North America. Our analysis is thus in agreement with the recent finding by Sung et al. (2019) that interdecadal La Niña-like conditions can enhance temperature extremes over North America through modulated baroclinic energy conversion of NPO anomalies, and we have confirmed that similar processes are operative also with interannual ENSO variability.

~~ENSO's modulation~~ induced anomalies of the extratropical circulation share ~~some~~ similarities with the PNA, but they are ~~is not perfectly the same~~ not identical (Straus and Shukla, 2002). ~~It is~~ The anomalies are ~~also~~ known, for instance, to be [projected also onto the Tropical Northern Hemisphere \(TNH\) pattern](#) (Soulard et al., 2019; Trenberth et al., 1998). [It remains unclear at this stage whether the modulation of baroclinic energy conversion is achieved through the projection of the extratropical response on the internally-driven PNA or TNH.](#) ~~but we~~ We nevertheless speculate that it may be achieved [primarily through the PNA, since important modulations of baroclinic energy conversion take place over the western North Pacific, where the PNA has a greater influence on the winter-mean flow. A more detailed investigation of the modulations of subseasonal energy sources by internally-generated interannual variability should be the topic of a future study. Nonetheless, we briefly investigated other factors that can affect subseasonal variability like ENSO.](#) ~~In addition to ENSO's influ and to fouind that~~ ~~ence~~, an important fraction of subseasonal SAT variability over North America appears related to interannual PNA-like or NPO-like atmospheric variability that is uncorrelated with ENSO. Our ability to forecast subseasonal variance
435 over North America may thus depend on the forecast skill of these other atmospheric teleconnections [seasons in advance](#) and thus on whether they are externally forced or purely internally generated.

[Concerning subseasonal predictions, our results suggest that predictive skill over North America may be deteriorated during La Niña winters due to enhanced energy conversion to subseasonal variability and, as a consequence, increased atmospheric internal variability over the sector. This is in agreement with the overall less skillful predictions achieved during the negative phase of the PNA](#) (Lin and Derome, 1996; Sheng, 2002) [which, in terms of extratropical mean flow changes, is to some extent similar to the extratropical response to La Niña.](#)
440

Code availability

The codes used in this paper can be obtained from the authors upon request.

445 Data availability

JRA-55 (Japan Meteorological Agency, 2013) was obtained from the NCAR/UCAR Research Data Archive (RDA). The HadISST dataset was obtained from the Met Office Hadley Centre.

Author contribution

450 All authors designed the analysis and edited the paper. PM performed the calculations, plotted the results, and drafted the original paper.

Competing interests

The authors declare that they have no conflict of interest.

Acknowledgements

455 This study is supported in part by the Japanese Ministry of Education, Culture, Sports, Science and Technology (MEXT) through the Arctic Challenge for Sustainability (ArCS/[ArCS-II](#)) Program and the Integrated Research Program for Advancing Climate Models (JPMXD0717935457), by the Japan Science and Technology Agency through Belmont Forum CRA “InterDec”, by the Japanese Ministry of Environment through Environment Research and Technology Development Fund 2-1904, and by the Japan Society for the Promotion of Science (JSPS) through Grants-in-Aid for Scientific Research JP16H01844, JP18H01278, JP18H01281, JP19H05702 and JP19H05703 (on Innovative Areas 6102). PM is partly
460 supported by Grant-in-Aid for JSPS Research Fellow.

References

- Alexander, M. A., Bladé, I., Newman, M., Lanzante, J. R., Lau, N.-C. and Scott, J. D.: The Atmospheric Bridge: The Influence of ENSO Teleconnections on Air–Sea Interaction over the Global Oceans, *J. Clim.*, 15(16), 2205–2231, doi:10.1175/1520-0442(2002)015<2205:TABTIO>2.0.CO;2, 2002.
- 465 Bamston, A. G., Chelliah, M. and Goldenberg, S. B.: Documentation of a highly ENSO-related sst region in the equatorial pacific: Research note, *Atmosphere-Ocean*, 35(3), 367–383, doi:10.1080/07055900.1997.9649597, 1997.
- Barnston, A. G. and Livezey, R. E.: Classification, Seasonality and Persistence of Low-Frequency Atmospheric Circulation

- Patterns, *Mon. Weather Rev.*, 115(6), 1083–1126, doi:10.1175/1520-0493(1987)115<1083:CSAPOL>2.0.CO;2, 1987.
- Barriopedro, D. and Calvo, N.: On the Relationship between ENSO, Stratospheric Sudden Warmings, and Blocking, *J. Clim.*, 27(12), 4704–4720, doi:10.1175/JCLI-D-13-00770.1, 2014.
- Bjornsson, H. and Venegas, S. A.: *A Manual for EOF and SVD Analyses of Climatic Data*, Department of Atmospheric and Oceanic Sciences and Centre for Climate and Global Change Research: McGill University, Montreal, Quebec., 1997.
- Blackmon, M. L., Madden, R. A., Wallace, J. M. and Gutzler, D. S.: Geographical Variations in the Vertical Structure of Geopotential Height Fluctuations 1, *J. Atmos. Sci.*, 36(12), 2450–2466, doi:10.1175/1520-0469(1979)036<2450:GVITVS>2.0.CO;2, 1979.
- Bretherton, C. S., Smith, C. and Wallace, J. M.: An Intercomparison of Methods for Finding Coupled Patterns in Climate Data, *J. Clim.*, 5(06), 541–560, doi:10.1175/1520-0442(1992)005<0541:AIOMFF>2.0.CO;2, 1992.
- Brunner, L., Schaller, N., Anstey, J., Sillmann, J. and Steiner, A. K.: Dependence of Present and Future European Temperature Extremes on the Location of Atmospheric Blocking, *Geophys. Res. Lett.*, 45(12), 6311–6320, doi:10.1029/2018GL077837, 2018.
- Buehler, T., Raible, C. C. and Stocker, T. F.: The relationship of winter season North Atlantic blocking frequencies to extreme cold or dry spells in the ERA-40, *Tellus, Ser. A Dyn. Meteorol. Oceanogr.*, 63(2), 212–222, doi:10.1111/j.1600-0870.2010.00492.x, 2011.
- Cai, M., Yang, S., Van Den Dool, H. M. and Kousky, V. E.: Dynamical implications of the orientation of atmospheric eddies: A local energetics perspective, *Tellus, Ser. A Dyn. Meteorol. Oceanogr.*, 59(1), 127–140, doi:10.1111/j.1600-0870.2006.00213.x, 2007.
- Cattiaux, J., Vautard, R., Cassou, C., Yiou, P., Masson-Delmotte, V. and Codron, F.: Winter 2010 in Europe: A cold extreme in a warming climate, *Geophys. Res. Lett.*, 37(20), n/a-n/a, doi:10.1029/2010GL044613, 2010.
- Chen, W. Y. and van den Dool, H. M.: Asymmetric Impact of Tropical SST Anomalies on Atmospheric Internal Variability over the North Pacific, *J. Atmos. Sci.*, 54(6), 725–740, doi:10.1175/1520-0469(1997)054<0725:AIOTSA>2.0.CO;2, 1997.
- Chen, W. Y. and Dool, H. M. Van Den: Significant change of extratropical natural variability and potential predictability associated with the El Niño/Southern Oscillation, *Tellus A Dyn. Meteorol. Oceanogr.*, 51(5), 790–802, doi:10.3402/tellusa.v51i5.14493, 1999.
- Compo, G. P., Sardeshmukh, P. D. and Penland, C.: Changes of Subseasonal Variability Associated with El Niño, *J. Clim.*, 14(16), 3356–3374, doi:10.1175/1520-0442(2001)014<3356:COVAV>2.0.CO;2, 2001.
- Dole, R. M.: Persistent Anomalies of the Extratropical Northern Hemisphere Wintertime Circulation: Structure, *Mon. Weather Rev.*, 114(1), 178–207, doi:10.1175/1520-0493(1986)114<0178:PAOTEN>2.0.CO;2, 1986.
- Gollan, G. and Greatbatch, R. J.: The relationship between Northern Hemisphere winter blocking and tropical modes of variability, *J. Clim.*, 30(22), 9321–9337, doi:10.1175/JCLI-D-16-0742.1, 2017.
- Hinton, T. J., Hoskins, B. J. and Martin, G. M.: The influence of tropical sea surface temperatures and precipitation on north Pacific atmospheric blocking, *Clim. Dyn.*, 33(4), 549–563, doi:10.1007/s00382-009-0542-7, 2009.

- Horel, J. D. and Wallace, J. M.: Planetary-Scale Atmospheric Phenomena Associated with the Southern Oscillation, *Mon. Wea. Rev.*, 109, 813–829, 1981.
- Kobayashi, S., Ota, Y., Harada, Y., Ebata, A., Moriya, M., Onoda, H., Onogi, K., Kamahori, H., Kobayashi, C., Endo, H.,
505 Miyaoka, K. and Takahashi, K.: The JRA-55 Reanalysis: General Specifications and Basic Characteristics, *J. Meteorol. Soc. Japan. Ser. II*, 93(1), 5–48, doi:10.2151/jmsj.2015-001, 2015.
- Lau, N.-C.: Interactions between Global SST Anomalies and the Midlatitude Atmospheric Circulation, *Bull. Am. Meteorol. Soc.*, 78(1), 21–33, doi:10.1175/1520-0477(1997)078<0021:IBGSAA>2.0.CO;2, 1997.
- Lau, N.-C. and Nath, M. J.: Variability of the Baroclinic and Barotropic Transient Eddy Forcing Associated with Monthly
510 Changes in the Midlatitude Storm Tracks, *J. Atmos. Sci.*, 48(24), 2589–2613, doi:10.1175/1520-0469(1991)048<2589:VOTBAB>2.0.CO;2, 1991.
- Lin, H.: Subseasonal variability of North American wintertime surface air temperature, *Clim. Dyn.*, 45(5–6), 1137–1155, doi:10.1007/s00382-014-2363-6, 2015.
- Lin, H. and Derome, J.: Changes in predictability associated with the PNA pattern, *Tellus A Dyn. Meteorol. Oceanogr.*,
515 48(4), 553–571, doi:10.3402/tellusa.v48i4.12139, 1996.
- Lin, H. and Derome, J.: On the modification of the high- and low-frequency eddies associated with the PNA anomaly: an observational study, *Tellus A Dyn. Meteorol. Oceanogr.*, 49(1), 87–99, doi:10.3402/tellusa.v49i1.12213, 1997.
- Linkin, M. E. and Nigam, S.: The North Pacific Oscillation-West Pacific teleconnection pattern: Mature-phase structure and winter impacts, *J. Clim.*, 21(9), 1979–1997, doi:10.1175/2007JCLI2048.1, 2008.
- 520 Lorenz, E. N.: Available Potential Energy and the Maintenance of the General Circulation, *Tellus*, 7(2), 157–167, doi:10.3402/tellusa.v7i2.8796, 1955.
- Di Lorenzo, E., Schneider, N., Cobb, K. M., Franks, P. J. S., Chhak, K., Miller, A. J., McWilliams, J. C., Bograd, S. J., Arango, H., Curchitser, E., Powell, T. M. and Rivière, P.: North Pacific Gyre Oscillation links ocean climate and ecosystem change, *Geophys. Res. Lett.*, 35(8), 2–7, doi:10.1029/2007GL032838, 2008.
- 525 Martineau, P., Chen, G. and Burrows, A. D.: Wave Events: Climatology, Trends, and Relationship to Northern Hemisphere Winter Blocking and Weather Extremes, *J. Clim.*, 30(15), 5675–5697, doi:10.1175/JCLI-D-16-0692.1, 2017.
- Mullen, S. L.: Model Experiments on the Impact of Pacific Sea Surface Temperature Anomalies on Blocking Frequency, *J. Clim.*, 2(9), 997–1013, doi:10.1175/1520-0442(1989)002<0997:MEOTIO>2.0.CO;2, 1989.
- Nakamura, H.: Year-to-Year and interdecadal variability in the activity of intraseasonal fluctuations in the Northern
530 Hemisphere wintertime circulation, *Theor. Appl. Climatol.*, 55(1–4), 19–32, doi:10.1007/BF00864700, 1996.
- Oort, A. H.: On Estimates Of The Atmospheric Energy Cycle, *Mon. Weather Rev.*, 92(11), 483–493, doi:10.1175/1520-0493(1964)092<0483:OEOTAE>2.3.CO;2, 1964.
- Pfahl, S. and Wernli, H.: Quantifying the relevance of atmospheric blocking for co-located temperature extremes in the Northern Hemisphere on (sub-)daily time scales, *Geophys. Res. Lett.*, 39(12), 1–6, doi:10.1029/2012GL052261, 2012.
- 535 Rayner, N. A., Parker, D. E., Horton, E. B., Folland, C. K., Alexander, L. V., Rowell, and D. P., Kent, E. C. and Kaplan, A.:

- Global analyses of sea surface temperature, sea ice, and night marine air temperature since the late nineteenth century, *J. Geophys. Res.*, 108(D14), 4407, doi:10.1029/2002JD002670, 2003.
- Renwick, J. a. and Wallace, J. M.: Relationships between North Pacific Wintertime Blocking, El Niño, and the PNA Pattern, *Mon. Weather Rev.*, 124(9), 2071–2076, doi:10.1175/1520-0493(1996)124<2071:RBNPWB>2.0.CO;2, 1996.
- 540 Rex, D. F.: Blocking Action in the Middle Troposphere and its Effect upon Regional Climate. I. An Aerological Study of Blocking Action, *Tellus*, 2, 196–211, doi:10.1111/j.2153-3490.1950.tb00331.x, 1950.
- Sheng, J.: GCM experiments on changes in atmospheric predictability associated with the PNA pattern and tropical SST anomalies, *Tellus A Dyn. Meteorol. Oceanogr.*, 54(4), 317–329, doi:10.3402/tellusa.v54i4.12153, 2002.
- Sheng, J. and Derome, J.: An observational study of the energy transfer between the seasonal mean flow and transient
545 eddies, *Tellus A*, 43(2), 128–144, doi:10.1034/j.1600-0870.1991.t01-1-00004.x, 1991.
- Sillmann, J., Mischa, C. M., Kallache, M. and Katz, R. W.: Extreme cold winter temperatures in Europe under the influence of North Atlantic atmospheric blocking, *J. Clim.*, 24(22), 5899–5913, doi:10.1175/2011JCLI4075.1, 2011.
- Simmons, a. J., Wallace, J. M. and Branstator, G. W.: Barotropic Wave Propagation and Instability, and Atmospheric
550 Teleconnection Patterns, *J. Atmos. Sci.*, 40(6), 1363–1392, doi:10.1175/1520-0469(1983)040<1363:BWPAIA>2.0.CO;2, 1983.
- Smith, C. A. and Sardeshmukh, P. D.: The effect of ENSO on the intraseasonal variance of surface temperatures in winter, *Int. J. Climatol.*, 20(13), 1543–1557, doi:10.1002/1097-0088(20001115)20:13<1543::AID-JOC579>3.0.CO;2-A, 2000.
- Soulard, N., Lin, H. and Yu, B.: The changing relationship between ENSO and its extratropical response patterns, *Sci. Rep.*, 9(1), doi:10.1038/s41598-019-42922-3, 2019.
- 555 Straus, D. M. and Shukla, J.: Does {ENSO} Force the {PNA}?, *J. Clim.*, 15, 2340–2358, 2002.
- Sung, M.-K., Jang, H.-Y., Kim, B.-M., Yeh, S.-W., Choi, Y.-S. and Yoo, C.: Tropical influence on the North Pacific Oscillation drives winter extremes in North America, *Nat. Clim. Chang.*, 9(5), 413–418, doi:10.1038/s41558-019-0461-5, 2019.
- Taguchi, S. and Asai, T.: Statistical Characteristics of Long-Lived Large-Scale Disturbances in the Northern Hemisphere
560 500hPa Height Fields, *J. Meteorol. Soc. Japan. Ser. II*, 65(2), 221–236, doi:10.2151/jmsj1965.65.2_221, 1987.
- Takaya, K. and Nakamura, H.: A formulation of a wave-activity flux for stationary Rossby waves on a zonally varying basic flow, *Geophys. Res. Lett.*, 24(23), 2985–2988, doi:10.1029/97GL03094, 1997.
- Takaya, K. and Nakamura, H.: A Formulation of a Phase-Independent Wave-Activity Flux for Stationary and Migratory Quasigeostrophic Eddies on a Zonally Varying Basic Flow, *J. Atmos. Sci.*, 58(6), 608–627, doi:10.1175/1520-
565 0469(2001)058<0608:AFOAPI>2.0.CO;2, 2001.
- Tam, C. Y. and Lau, N. C.: The impact of ENSO on atmospheric intraseasonal variability as inferred from observations and GCM simulations, *J. Clim.*, 18(12), 1902–1924, doi:10.1175/JCLI3399.1, 2005.
- Tanaka, S., Nishii, K. and Nakamura, H.: Vertical structure and energetics of the Western Pacific teleconnection pattern, *J. Clim.*, 29(18), 6597–6616, doi:10.1175/JCLI-D-15-0549.1, 2016.

570 Trenberth, K. E., Branstator, G. W., Karoly, D., Kumar, a, Lau, N. C. and Ropelewski, C.: Progress during TOGA in understanding and modeling global teleconnections associated with tropical sea surface temperatures, J. Geophys. Res., 103(C7), 14291–14324, doi:10.1029/97jc01444, 1998.

Wallace, J. M. and Gutzler, D. S.: Teleconnections in the Geopotential Height Field during the Northern Hemisphere Winter, Mon. Weather Rev., 109(4), 784–812, doi:10.1175/1520-0493(1981)109<0784:TITGHF>2.0.CO;2, 1981.

575

Table 1: Pairwise correlation coefficients between SVD1_{SSV}, SVD1_{SST}, and the Niño indices (described in section 0). Correlations that are significant at the 95% confidence level are indicated in boldface. ~~All correlations are significant at the 95% confidence level.~~

580

	SVD1 _{SST}	Niño1+2	Niño3	Niño3.4	Niño4	SVD1 _{SST}	Niño1+2	Niño3	Niño3.4	Niño4
SVD1 _{SSV}	0.46	-0.38	-0.42	-0.39	-0.23	0.54	-0.35	-0.39	-0.37	-0.22
SVD1 _{SST}		-0.83	-0.96	-0.94	-0.80		-0.79	-0.93	-0.90	-0.76

Table 2: Pairwise correlation coefficients between SVD1_{RSSV} and the Niño indices (described in section 0). Correlations that are significant at the 95% confidence level are indicated in boldface.

585

	Niño1+2	Niño3	Niño3.4	Niño4	Niño1+2	Niño3	Niño3.4	Niño4
SVD1 _{RSSV}	0.09	0.13	0.14	0.23	0.00	0.03	0.04	0.15

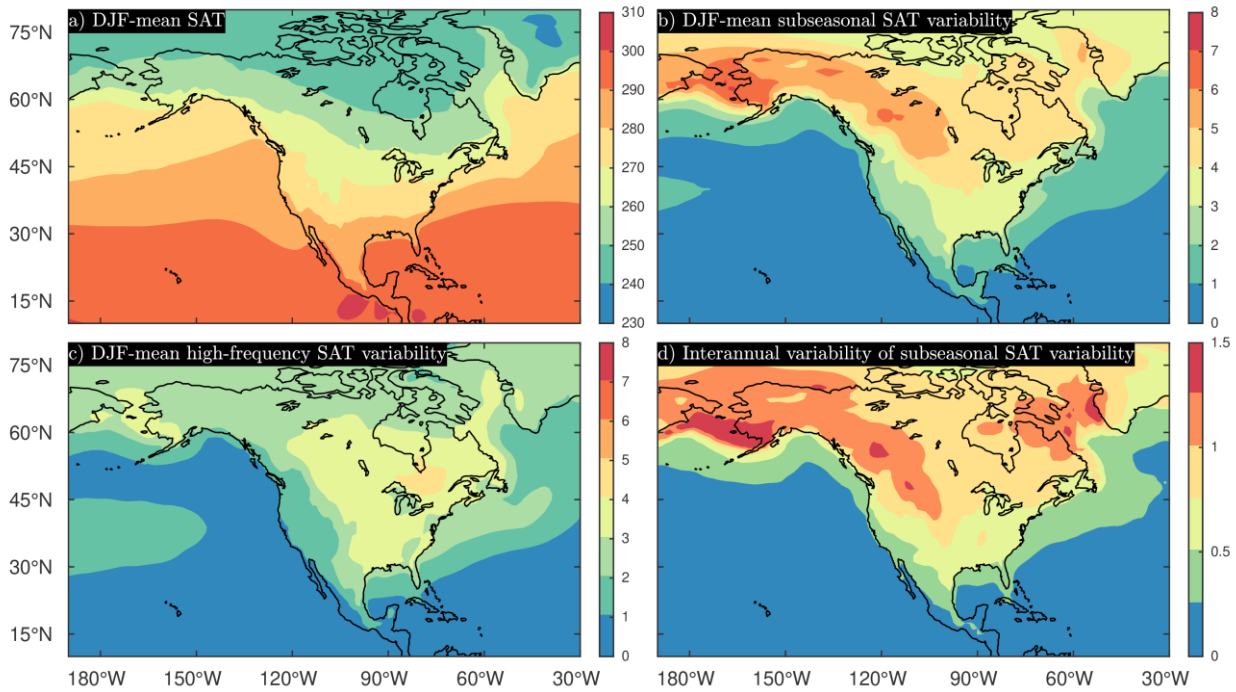


Figure 1: Climatological features of SAT variability (1958-2015). The a) DJF-mean SAT, b) DJF-mean subseasonal SAT variability, or SSV, c) DJF-mean high-frequency SAT variability, and d) interannual modulations of subseasonal SAT variability are shown with colour shadings. All variables are in units of K. Variability is illustrated with the standard deviation.

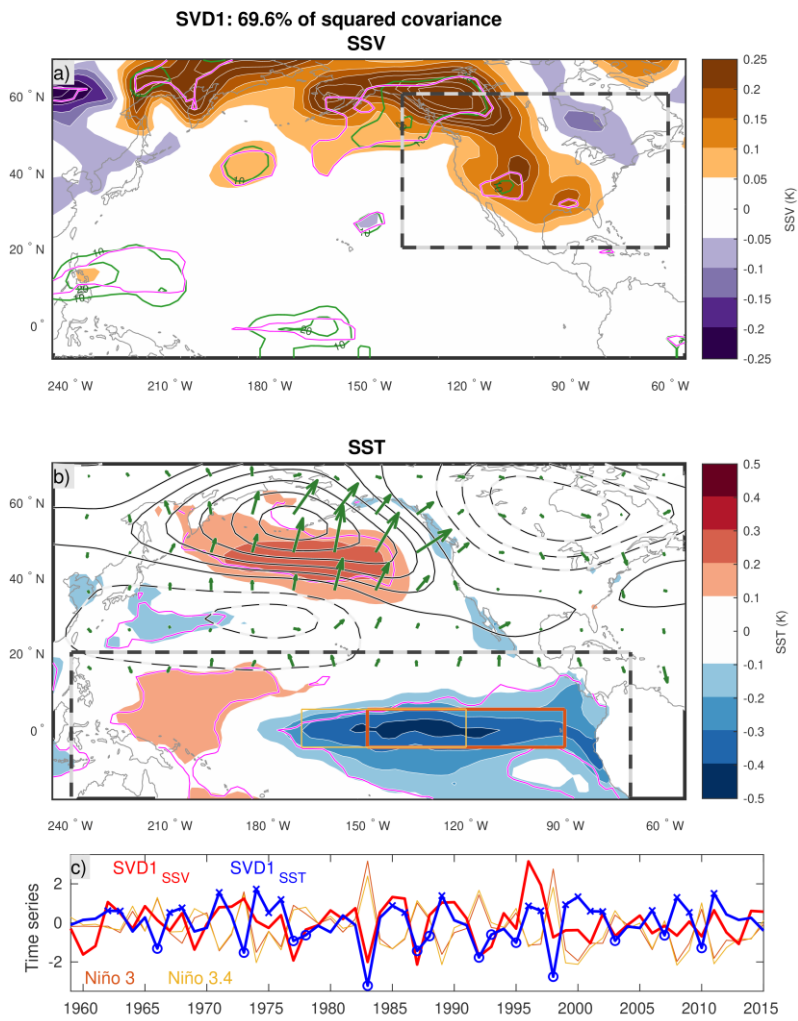


Figure 2: Wintertime anomaly patterns of a) SSV (subseasonal SAT variability) and b) winter-mean SST associated with the dominant mode of covariability (SVD1, corresponding to La Niña) between the two variables (color shadings; anomalies statistically significant at the 95% level are contoured in magenta). The sectors used for the SVD analysis are bounded by bold dashed lines. The green contours superimposed on a) indicate the fractional change of SSV relative to the climatology fraction of interannual SSV variability explained by this mode with 10% contour intervals (solid and dashed contours are used for positive and negative values, respectively; the 0 line is omitted). Z500 anomalies regressed onto SVD1_{SST} are superimposed on b) with black contours (increment of 5 m, solid and dashed for positive and negative anomalies, respectively). The corresponding wave-activity fluxes (Takaya and Nakamura, 2001) are shown with green arrows. A distance of 1° corresponds to a flux of 0.125 m² s⁻². c) Anomaly time series of SSV (SVD1_{SSV}, red) and SST (SVD1_{SST}, blue) associated with SVD1. Two Niño indices are superimposed (domains used to compute these indices are illustrated over the SST pattern in b).

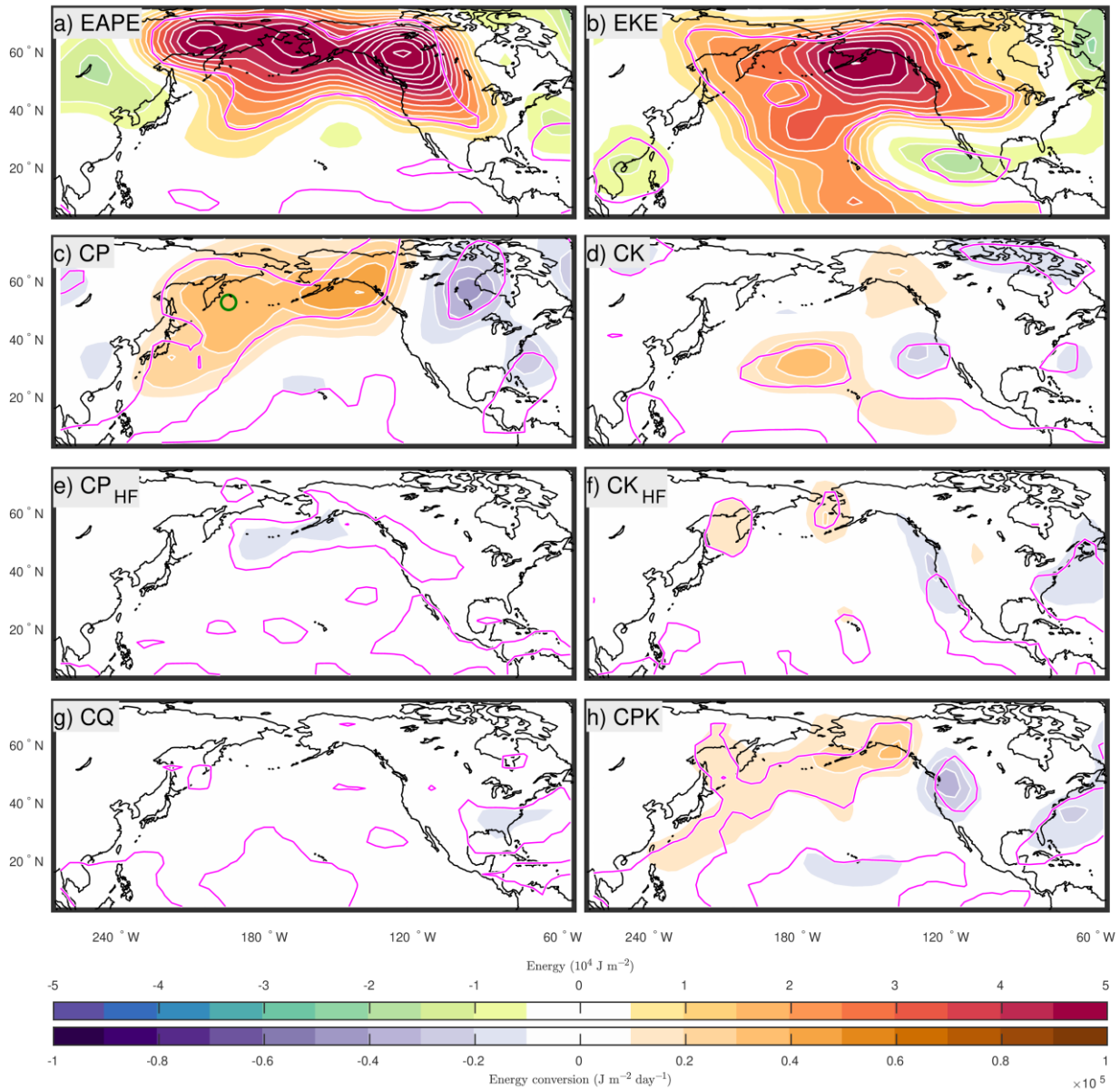
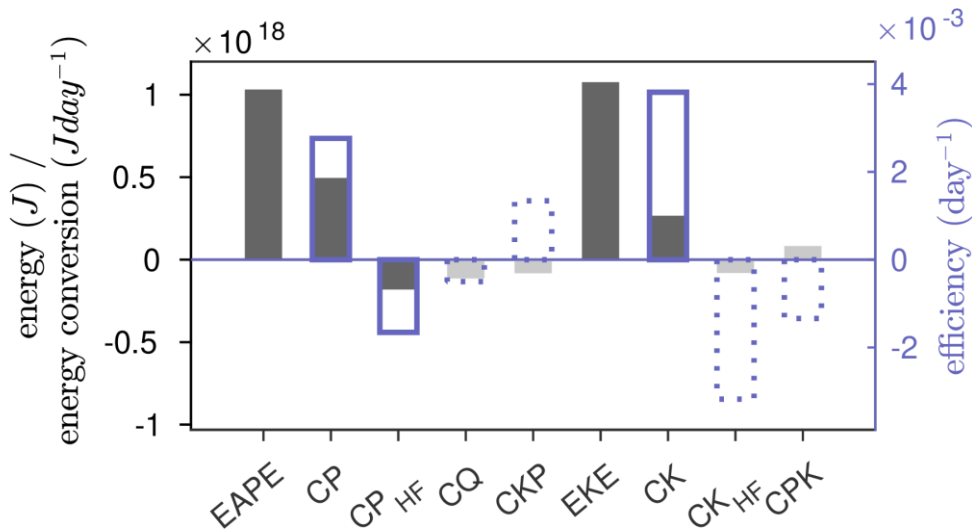
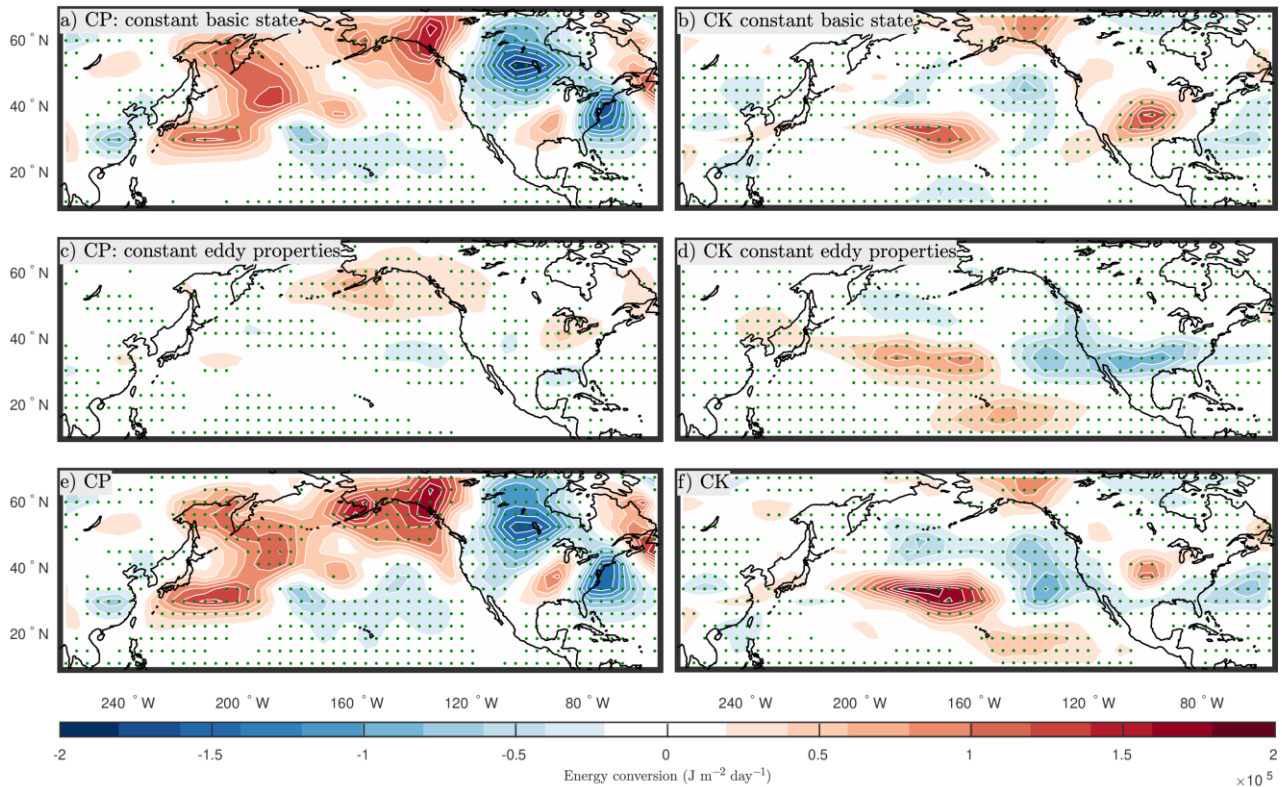


Figure 23: The a) eddy available potential energy (EAPE) and b) eddy kinetic energy (EKE) of subseasonal eddies and energy sources/sinks (c-h) are regressed onto the SVD1SSR index. CP and CK are the baroclinic and barotropic energy conversions, respectively. CP_{HF} and CK_{HF} represent the baroclinic and barotropic high-frequency eddy feedbacks. CQ is the diabatic feedback. CPK represents transfers from EAPE to EKE. Correlations that are statistically significant at the 95% confidence level are contoured in magenta.

605



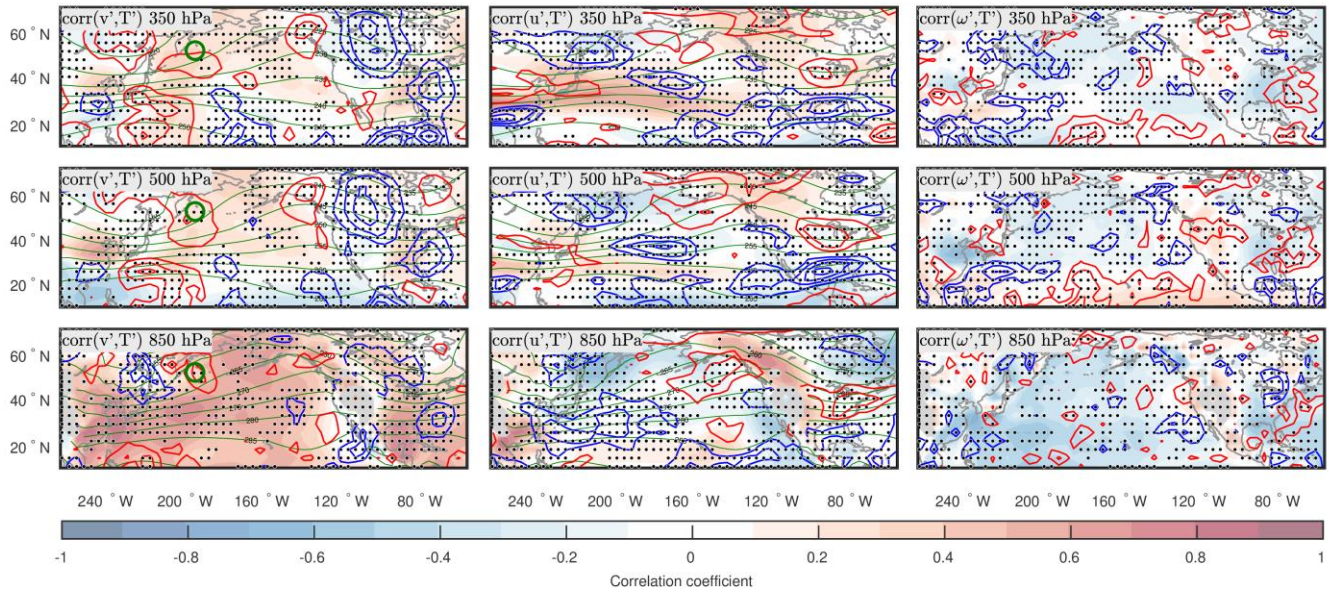
610 **Figure 34:** The energetics of subseasonal eddies are integrated over the North Pacific (0° - 87.5° N, 120° E- 55° W) and regressed onto SVD1_{SST}. Raw changes in energy and sources/sinks are shown with solid bars. Significant values are shown with a darker shade of grey. Blue boxes indicate changes in the efficiency with significant changes indicated with solid borders. [Quantities shown include eddy available potential energy \(EAPE\), baroclinic energy conversion \(CP\), high-frequency eddy baroclinic feedback \(CP_{HF}\), diabatic feedback \(CQ\), transfers from EKE to EAPE \(CKP\), eddy kinetic energy \(EKE\), barotropic energy conversion \(CK\), high-frequency barotropic feedback \(CK_{HF}\), and transfers from EAPE to EKE \(CPK\).](#)



615

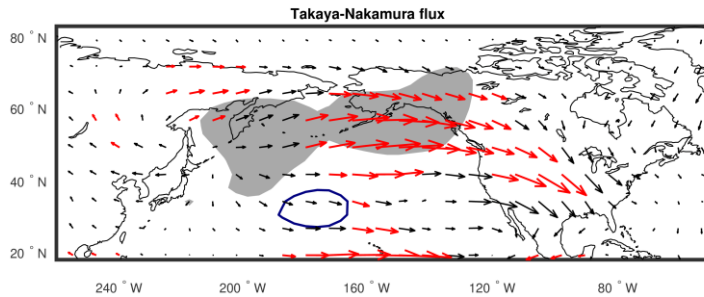
Figure 45: Baroclinic energy conversion (CP; left) and barotropic energy conversion (CK; right) composite differences between the positive and negative phases of SVD1 (representing La Niña) are calculated by keeping either the background flow properties (a, b) or eddy properties (c,d) constant every year. For reference, the composite difference when both eddy properties and the basic state can change from year to year is shown in e) and f). Composite differences that are significant at the 90% confidence level are dotted.

620



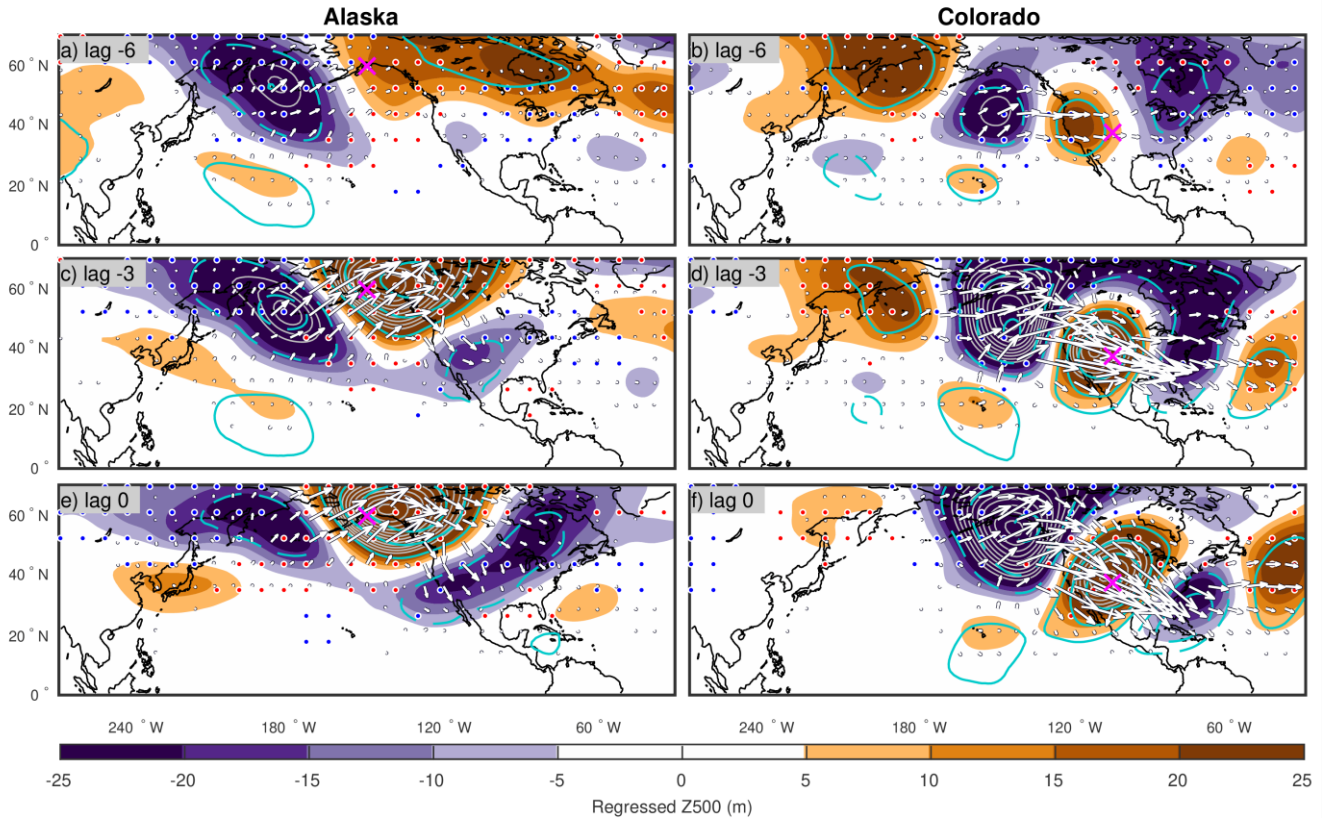
625

Figure 56: Maps of climatological Composite differences of correlation coefficients (colour shading) between (left) between v' and T' , (centre) between u' and T' , and (right) between ω' and T' . The respective composite differences between winters of $SVD1_{SST} > 0.5$ and $SVD1_{SST} < -0.5$. The composite difference is shown with are superimposed with blue and red contours with an interval of 0.1 for negative and positive values differences, respectively. The climatological correlation is shown with colour shadings. For reference, the temperature climatology is shown with green lines. Composite differences that are significant at the 90% confidence level are dotted.



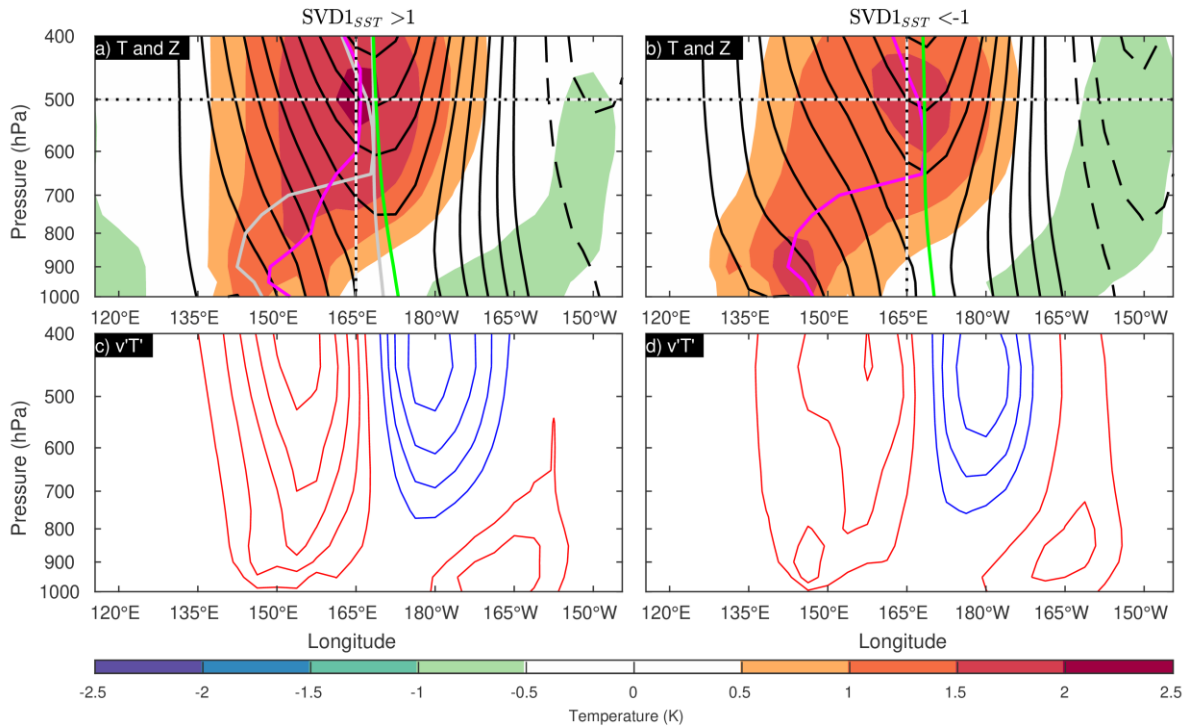
630

Figure 67: The wave-activity flux (Takaya and Nakamura, 2001) of 10-60 day band-pass-filtered eddies at 500 hPa regressed onto the $SVD1_{SST}$ time series. The anomalous flux whose meridional or vertical component is significant at the 95% level, assessed with a t-test on the correlation coefficients, are shown in red. A distance of 1° corresponds to a flux of $0.67 \text{ m}^2 \text{ s}^{-2}$. Regions where CP and CK are larger than $3 \times 10^4 \text{ J m}^{-2} \text{ day}^{-1}$ are denoted with grey shading and a blue contour, respectively (see Figs. 2c-d).



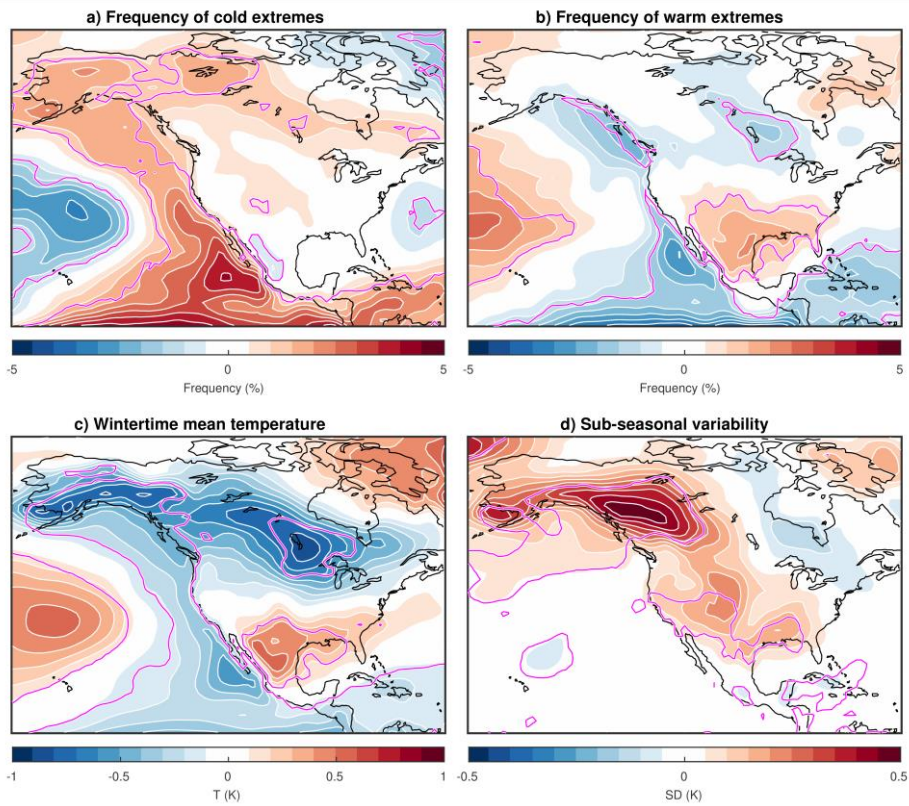
635 **Figure 7:** One-point regression maps of Z500 anomalies (colour shading) with respect to reference SAT time series over (left) Alaska (61°N, 150°W) and (right) Colorado (39°N, 105°W). The corresponding correlation is superimposed with cyan contours (increments of 0.2). The regression is performed separately for years when $SVD1_{SST} \geq 1$ and $SVD1_{SST} \leq -1$ (indicated with blue crosses and circles in Fig. 1, respectively) and the average of the two patterns is shown in this figure. The reference SAT time series for the positive and negative phases are normalized independently before carrying out the regression. Differences between the $SVD1_{SST} \geq 1$ and $SVD1_{SST} \leq -1$ patterns that are significant at the 95% level are shown with blue dots for negative differences and red dots for positive differences. The wave-activity flux (Takaya and Nakamura, 2001) evaluated with the regressed Z500 anomalies is shown with white arrows with a distance of 1° corresponding to a flux of $2/3 \text{ m}^2 \text{ s}^{-2}$.

640



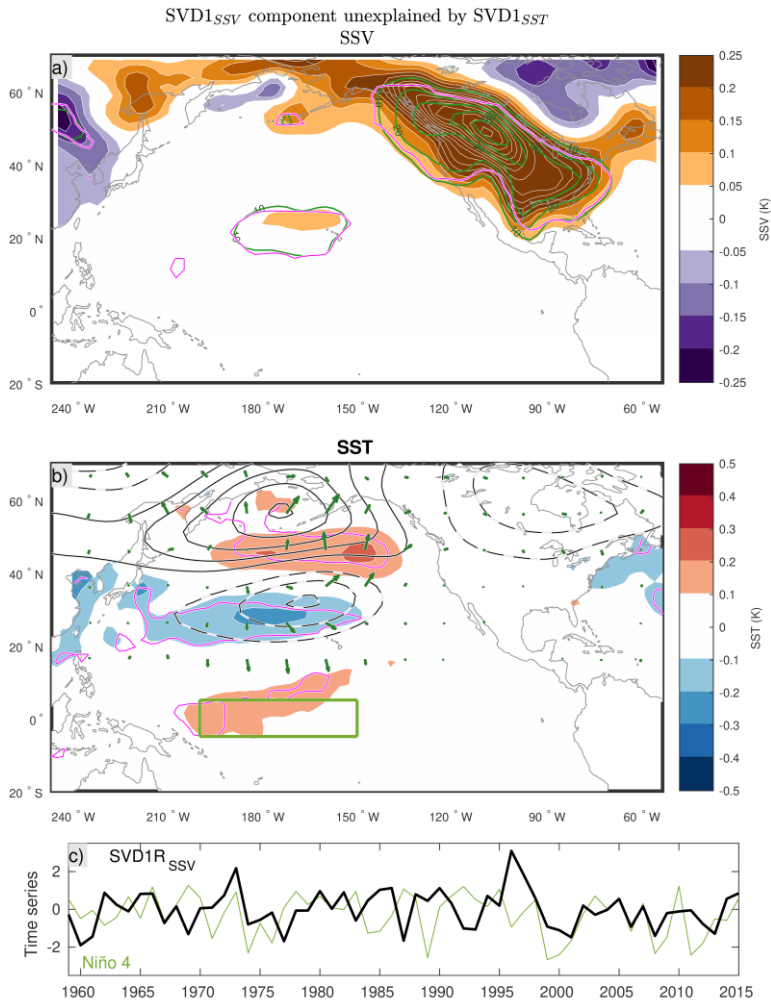
645

Figure 98: (a, b) Zonal sections of subseasonal anomalies in anomalies of geopotential height anomalies (black contours with intervals of 10 m; solid and dashed lines are used for positive and negative values, respectively) and temperature (shadings) both regressed onto the reference time series of geopotential height at [53.4°N, 165.575°W] (green circles on Figs. 3c and 6), for winters when (a: left) $SVD1_{SST} > 1$ and (b: right) $SVD1_{SST} < -1$. The maxima of the geopotential height and temperature anomalies at every individual pressure levels are linked-connected vertically with green and magenta lines, respectively. The lines shown in b) are also repeated in grey in a) for comparison. (c, d) The associated meridional heat fluxes ($v'T'$) are contoured at intervals of 1 m K s⁻¹ with red and blue lines for positive (northward) and negative (southward) values, respectively.



650

Figure 109: Regression of a) frequency of cold extremes, b) frequency of warm extremes, c) winter-mean SAT, and d) subseasonal SAT variability onto the SVD1_{SST} index. Values that are statistically significant at the 95% confidence level are contoured in magenta.



655 Figure 110: SSV a) and SST b) are regressed on the component of SVD1_{SSV} that is not correlated with SVD1_{SST} (SVD1R_{SSV}). Regions that are statistically significant at the 95% level are contoured in magenta. The green contours superimposed on a) indicate the fraction of interannual SSV variability explained by this mode ~~fractional change of SSV relative to the climatology~~ with 10% contour intervals (solid and dashed contours are used for positive and negative values, respectively; the 0 line is omitted). The regression of Z500 (contours, 5 m intervals with solid and dashed black contours for positive and negative anomalies) is also shown in panel b). The corresponding wave-activity fluxes (Takaya and Nakamura, 2001) are shown with green arrows. A distance of 1° corresponds to a flux of 0.125 m² s⁻². The SVD1R_{SSV} time series, as well as the the four Niño 4 indices considered index, are shown in c) and the regions used to compute these this indices index are is illustrated over the SST pattern in b).

660